

**Stem Cell Reports, Volume 16**

**Supplemental Information**

**Non-viral Induction of Transgene-free iPSCs from Somatic Fibroblasts  
of Multiple Mammalian Species**

**Sho Yoshimatsu, Mayutaka Nakajima, Aozora Iguchi, Tsukasa Sanosaka, Tsukika Sato, Mari Nakamura, Ryusuke Nakajima, Eri Arai, Mitsuru Ishikawa, Kent Imaizumi, Hirotaka Watanabe, Junko Okahara, Toshiaki Noce, Yuta Takeda, Erika Sasaki, Rüdiger Behr, Kazuya Edamura, Seiji Shiozawa, and Hideyuki Okano**

## Supplemental Notes

### Note S1. Induction of marmoset primordial germ cell-like cells (PGCLCs) (related to Figure S5).

For PGCLC induction, since our preliminary attempts with only cytokines (BMP4, SCF, EGF and LIF) were unsuccessful, we exploited the combinatorial usage of the dexamethasone/doxycycline-inducible *SOX17/BLIMP1* overexpression system and cytokines (BMP4, SCF, EGF and LIF) (Figure S5C–D) (Supplementary Methods) according to the reported methods in previous studies on PGCLC induction from human and porcine PSCs (Gao et al., 2019; Kobayashi et al., 2017).

However, compared to the BLIMP1-Venus-positive rates of Day10-differentiated cells from marmoset ESCs (Figure S5E–F; ~50% from No. 40 ESCs and ~40% from DSY127 ESCs), the BLIMP1-Venus-positive rate of Day10-differentiated cells from marmoset iPSC (E01F A-2-2) was extremely low (Figure S5 E–F; 1–2%). Nevertheless, by mRNA-seq analysis, we discovered the PGCLCs (BLIMP1-Venus-positive cells on Day 10) from both of marmoset ESCs and iPSCs were plotted together in PCA (Figure S5G).

Compared to marmoset ESCs and iPSCs, the resultant PGCLCs showed enhanced expression of PGC specification markers, including *SOX17*, *PRDM1* (*BLIMP1*), *NANOS3*, *SOX15*, *KIT*, *ALPL* and *TFAP2C* (Figure S5H–I). In addition, the marmoset PGCLCs showed sustained expression of pluripotency-related genes such as *POU5F1* (*OCT4*), *UTF1*, *NANOG*, and *LIN28A*, while *SOX2* expression was significantly decreased (Figure S5H–I), which is consistent with previous findings on primate PGCs and PGCLCs (Irie et al., 2015; Sasaki et al., 2016; Sasaki et al., 2015), but clearly distinct from mouse PGCs (Campolo et al., 2013; Ohinata et al., 2009).

Moreover, by differential expressed gene (DEG) analysis of PGCLCs and PSCs (Figure S5I and Supplemental Table 1), we discovered significantly upregulated cell-surface markers including *KIT* (CD117) and *CXCR4* (CD184), which may make it possible to monitor marmoset PGCLC differentiation without the usage of genetic reporters. RNA from a whole testis of an adult marmoset (Adult\_Testis) was used as a positive control for mature germ cell markers, including *DDX4*, *DAZL*, *PIWIL1*, *PIWIL4*, *SYCP3* and *SYCP1* (Figure S5I). Although DSY127 ESC/E01F iPSC-derived PGCLCs showed a marginal increase in the expression of *DDX4*, other markers were not upregulated in all PGCLC samples (Figure S5I).

**Note S2. The high neurogenic potential of iNSLCs (related to Figure S6).**

To analyze the neurogenic potential of the iNSLCs, we performed a direct neurosphere formation assay (Yoshimatsu et al., 2019a) using the MHM medium, which supports neuronal survival without restricting differentiation toward other cell lineages. The marmoset iNSLCs, iPSCs and ESCs were cultured in suspension for one week, followed by further differentiation in an adherent culture (Figure S6G).  $\beta$ III-tubulin(+) neurons were not derived from the ESCs and iPSCs using this method (Figure S6H), which was consistent with previous observations (Yoshimatsu et al., 2019a). Surprisingly, under the same condition,  $\beta$ III-tubulin(+) neurons were derived from iNSLCs with 14–78% efficiency (Figure S6H–I). The iNSLCs showed various degrees of cell viability and neuronal differentiation efficiency following differentiation, which may be due to the differential ectopic expression levels of the remaining transgenes (Figure 4F). Among the iNSLCs, I5061F B-0 iNSLCs showed the highest efficiency of neuronal differentiation, which we decided to use for further differentiation assays.

To investigate the gliogenic potential of the iNSLC, day 7 primary neurospheres were dissociated into single cells and cultured in suspension for an additional week for the formation of secondary neurospheres, which was followed by further differentiation in an adherent culture. As a result, we observed ~ 30% GFAP-positive glial cells among the total population of cells (Figure S6J).

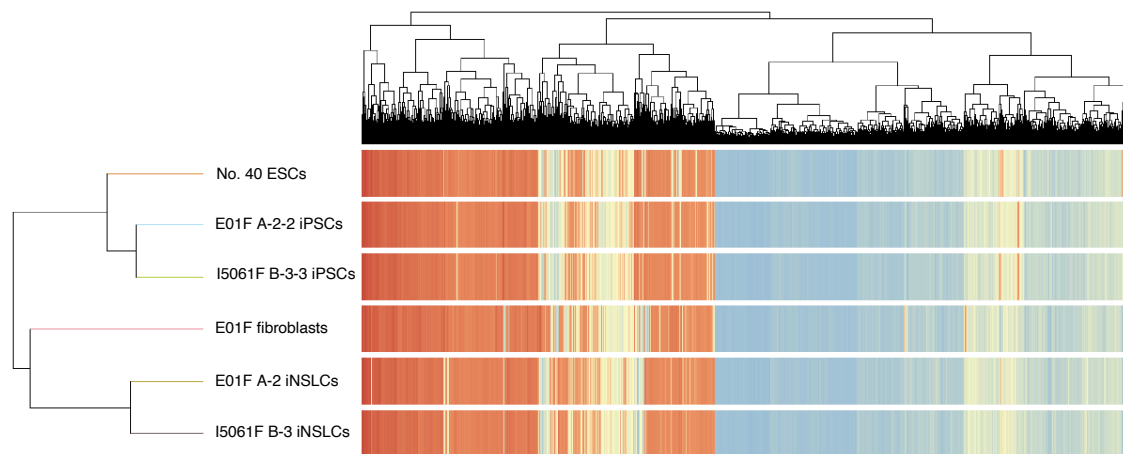
It was previously reported that the regional identity of induced neural progenitors derived from primate fibroblasts by ectopic expression of *OCT4*, *SOX2*, *KLF4* and *C-MYC* can be controlled by the supplementation of morphogens that are critical for neural development (Lu et al., 2013). When testing various morphogens, we succeeded in the posteriorization/ventralization of the iNSLCs by supplementation of retinoic acid, WNT agonist CHIR99021, and SHH agonist Purmorphamine to the medium during secondary neurosphere formation, which resulted in the emergence of ChAT/Islet1-positive motor neurons (~ 20% double-positive neurons out of the total population of cells; Figure S6K), and ~ 1% Galactocerebroside (GalC)-positive oligodendrocytes (Figure S6L).

**Note S3. Microarray analysis of marmoset fibroblasts, iNSLCs, ESCs and iPSCs.**

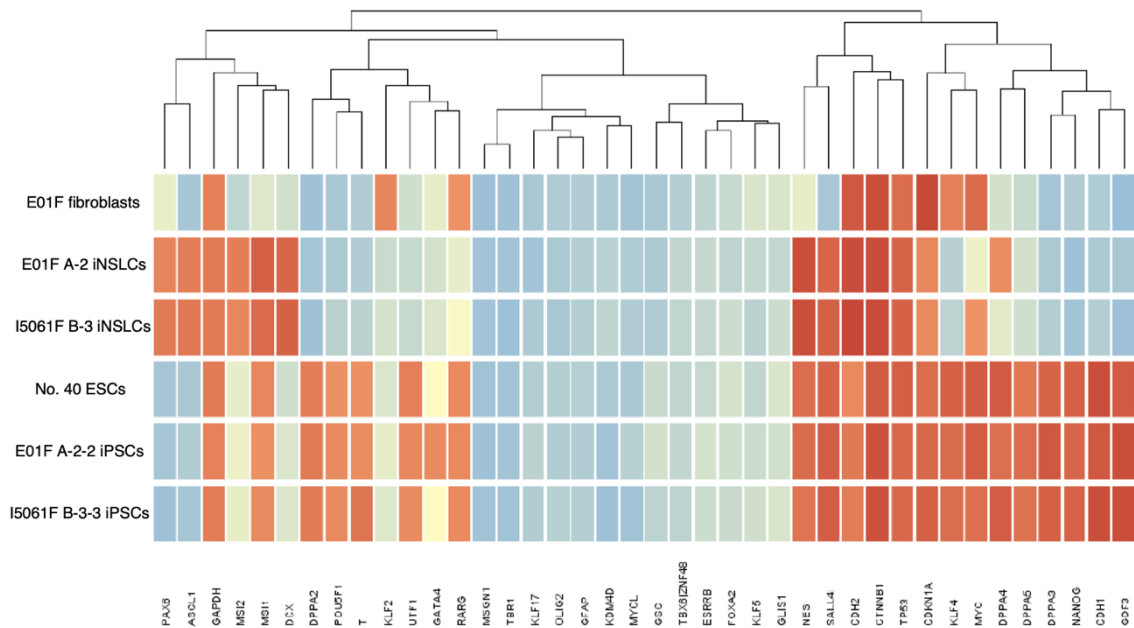
To elucidate the global differences and similarities of gene expression among these cells, we performed transcriptomic analyses by 3'IVT microarray. We used total RNA extracted

from the following six samples: embryonic marmoset fibroblasts (E01F fibroblasts), embryonic marmoset iPSCs (E01F A-2-2 iPSCs), embryonic marmoset iNSLCs (E01F A-2 iNSLCs), adult marmoset iPSCs (I5061F B-3-3 iPSCs), adult marmoset iNSLCs (I5061F B-3 iNSLCs) and marmoset ESCs (No.40 ESCs). The iNSLC clones, E01F A-2 and I5061 B-3, were parental of the iPSC clones, E01F A-2-2 and I5061F B-3-3, respectively.

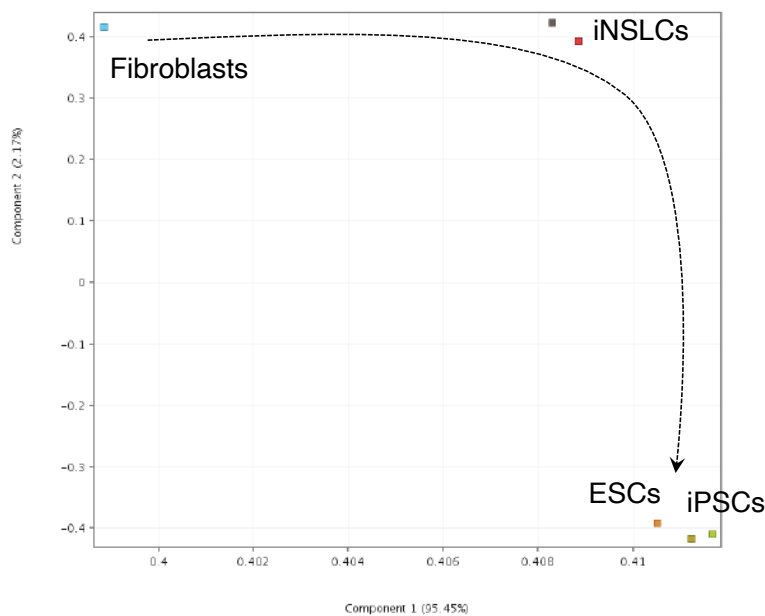
By hierarchical clustering of global gene expression as shown below, we found that the PSCs (ESCs and iPSCs), fibroblasts, and iNSLCs were clearly distinguished from each other.



In addition, when looking at individual genes (shown below), we detected high expression of NSC markers *PAX6*, *ASCL1*, *MSI* and *MSI2* in the iNSLCs, which correlated with the results of the qPCR analysis (Figure 4G). Meanwhile, PSC markers *DPPA2*, *POU5F1* (*OCT4*), *UTF1*, *RARG*, *DPPA5*, *NANOG* and *GDF3* were specifically expressed in the PSCs, but not in the iNSLCs (Figure S7B). Notably, *SALL4* was strongly expressed in both iNSLCs and PSCs, but not in the fibroblasts (Figure S7B). Hou *et al.* reported that during a chemical compound-based reprogramming of murine fibroblasts toward pluripotency, *SALL4* expression was upregulated along with pluripotency-related marker genes at the initial stages of the reprogramming process (Hou *et al.*, 2013). Importantly, some of these compounds (Forskolin, CHIR99021 and 616452 (TGF- $\beta$  inhibitor)) were also supplemented in the NSM of our study, which may be why *SALL4* was upregulated in the iNSLCs. On the other hand, we did not detect any *SALL4* expression in the *in vivo*-derived NSCs (data not shown). Thus, the high expression of *SALL4* in the iNSLCs may suggest that the iNSLC state reflects an early phase of the reprogramming process toward pluripotency.



Furthermore, by principal component analysis (PCA) of the 6 types of cells (shown below), fibroblasts and the other 5 types of cells were clearly separated by component 1 (95.45%). Additionally, iNSLCs and PSCs were clearly separated by component 2 (2.17%).



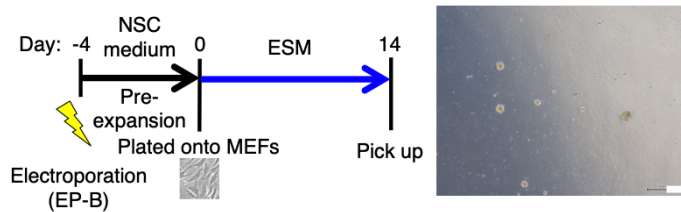
Color by Samples

E01F fibroblast.CEL	E01F A-2 iNSLC.CEL	E01F A-2-2 iPSC.CEL	I5061F B-3 iNSLC.CEL	I5061F B-3-3 iPSC.CEL
No.40 ESC.CEL				

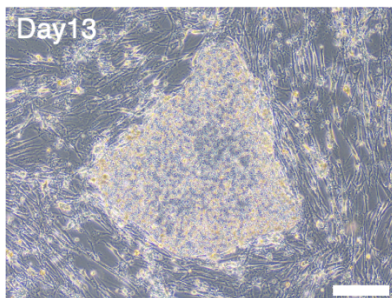
**Note S4. Reprogramming of marmoset *in vivo*-derived NSCs toward a pluripotent state.**

To investigate an iPSC-reprogramming potential of marmoset NSCs, we used primary

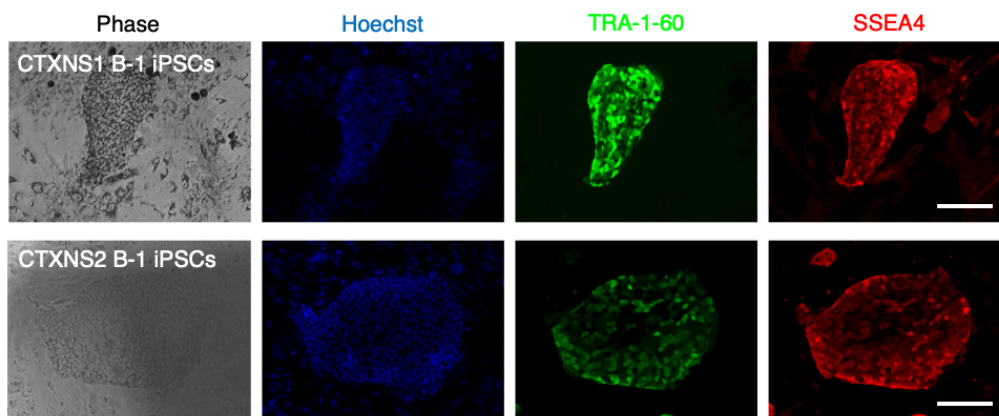
NSCs derived from the biopsy of cerebral cortexes from two embryonic marmosets (named CTXNS1 and CTXNS2). We transfected the EP-B vector set (Figure 1A, bottom) into the NSCs, pre-expanded them in MHM medium for four days (as shown below right, white scale bar = 200  $\mu$ m), and plated them onto MEFs using ESM.

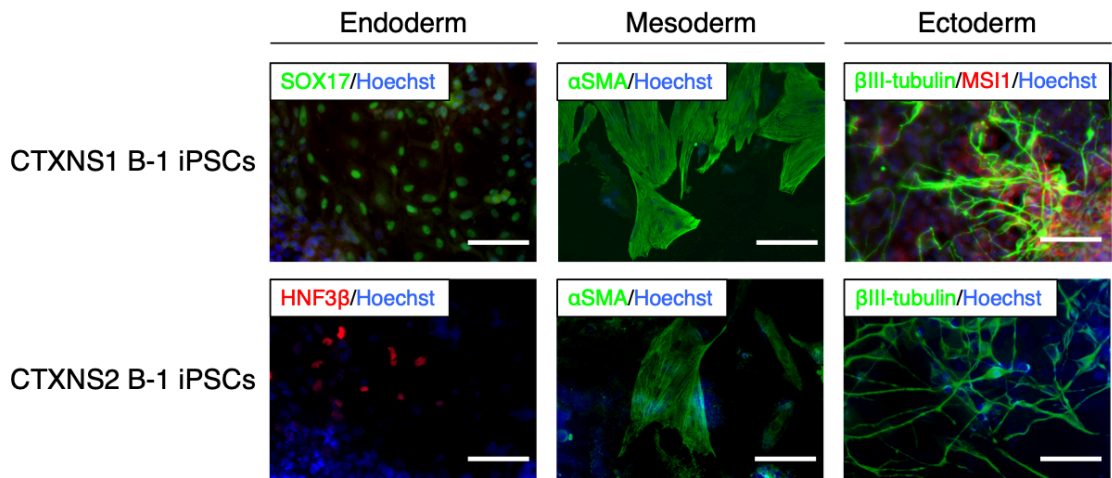


Surprisingly, although we could not induce colony formation from marmoset fibroblasts with ESM, we succeeded in deriving putative iPSC colonies (a representative colony on day 13 is shown below, scale bar = 200  $\mu$ m) from the NSCs at an efficiency of  $0.055 \pm 0.012\%$  ( $n = 2$ , independent experiments using NSCs from two marmosets).



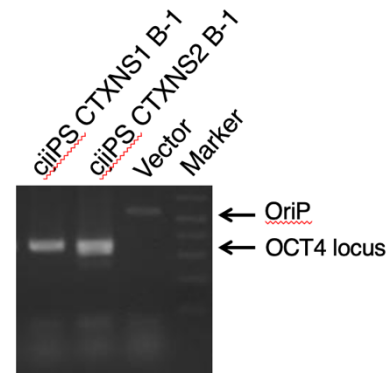
Using one putative iPSC clone from each marmoset (CTXNS1 B-1 and CTXNS2 B-1), we confirmed pluripotency marker expression (scale bars = 100  $\mu$ m) as shown below. In addition, we confirmed the three-germ-layer differentiation potential of the NSC-derived iPSCs (scale bars = 100  $\mu$ m) as shown below.





Also, by genomic PCR analysis, we found the removal of episomal vectors from the iPSCs at passage 5 as shown on the right, and female origin of both the iPSC lines were confirmed (Figure S4C).

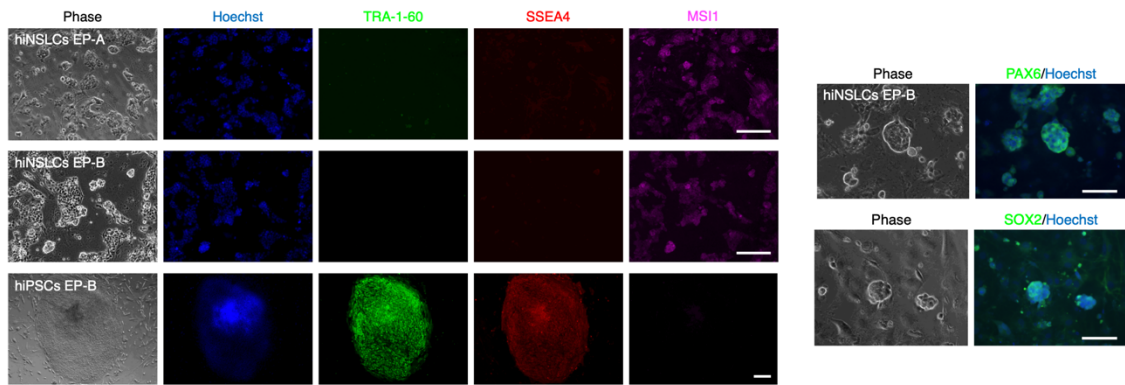
Reprogramming of NSCs toward a pluripotent state has been previously reported using mouse (Di Stefano et al., 2009; Kim et al., 2008) and human cells (Kim et al., 2009a), but among these reports, there was a variation in iPSC derivation efficiency compared to the reprogramming of fibroblasts (Di Stefano et al., 2009; Kim et al., 2009a; Kim et al., 2008). In contrast, we clearly demonstrated that marmoset NSCs can be reprogrammed to iPSCs more efficiently than fibroblasts (Figure 1). Thus, the transcriptional similarity of the iNSLCs to NSCs may provide an explanation for the successful conversion of the iNSLCs into a pluripotent state.



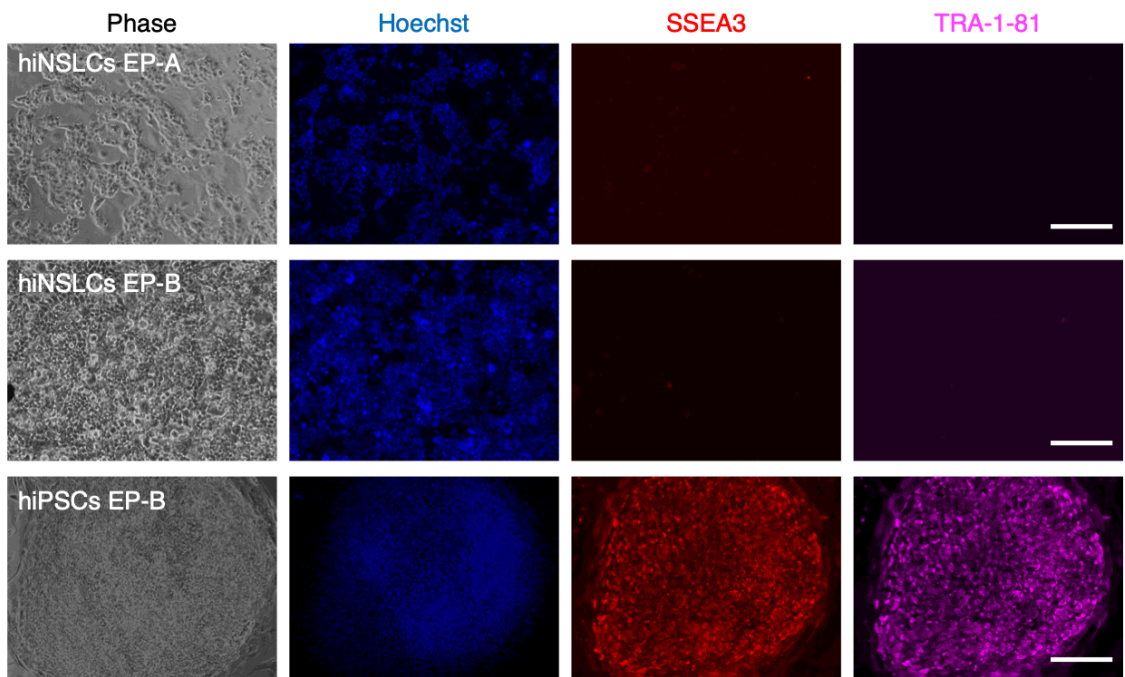
#### Note S5. Derivation of human iNSLCs.

To validate the applicability of our reprogramming methodology to somatic fibroblasts of other species beside marmosets, we attempted to reprogram human Bj fibroblasts using the same method. Following transfection of the EP-A or EP-B vector set and induction using NSM for three weeks, we observed the emergence of primary colonies, which were positive for MS11, SOX2 and PAX6 (as shown below, scale bars = 100  $\mu$ m).

But these cells were negative for representative human PSC markers such as TRA-1-60, SSEA4, SSEA3 and TRA-1-81 (as shown below, scale bars = 100  $\mu$ m).



This was quite distinct from hiPSCs, which were derived from Bj fibroblasts using a conventional iPSC medium and EP-B vector set. When using the EP-B vector set, the derivation efficiency of primary iNSLC colonies using NSM was  $0.016 \pm 0.002\%$  ( $n = 3$ , independent experiments), which was significantly higher than that when using a conventional hiPSC medium,  $0.003 \pm 0.002\%$  ( $n = 3$ , independent experiments).



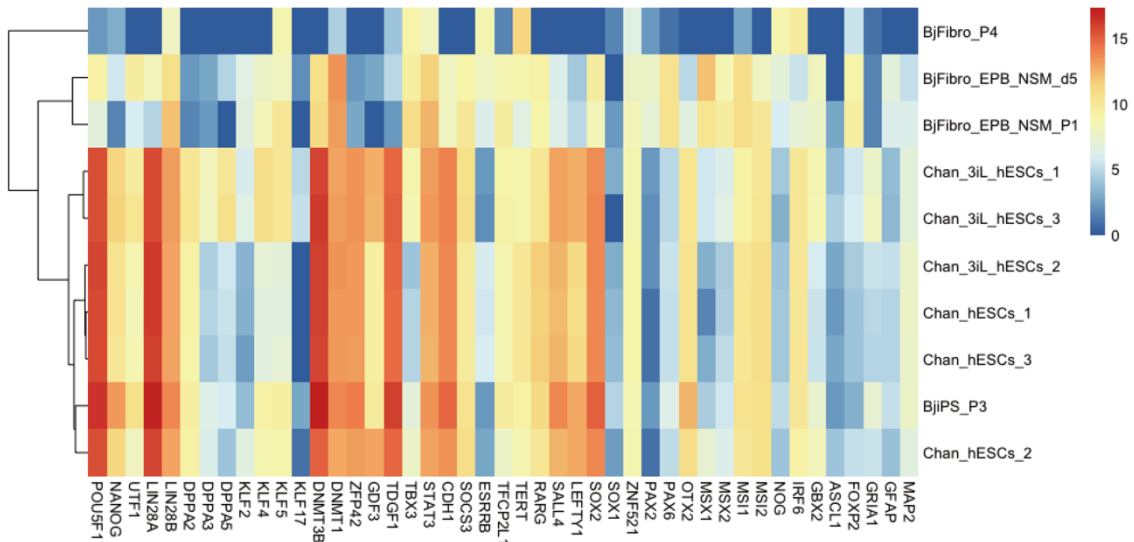
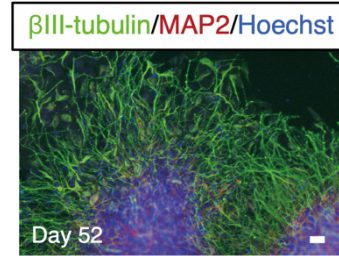
To assess the neural differentiation potential of the human iNSLCs, we performed the direct neurosphere formation assay (Note S2 and Figure S6G) (Yoshimatsu et al., 2019a). Although few cells (less than 1%) differentiated into  $\beta$ III-tubulin-positive neurons by the original protocol (data not shown), prolonged adherent culture (1.5 month) resulted in robust neural differentiation ( $\sim 80\%$   $\beta$ III-tubulin and MAP2-double positive cells; as shown in the right, scale bar =  $100 \mu\text{m}$ ), showing their high neural differentiation potential



and comparatively slower differentiation kinetics than that of marmoset iNSLCs.

Moreover, we performed mRNA-seq using RNA from human samples including Bj fibroblast-derived iNSLCs (BjFibro\_EPB\_NSM\_d5 and P1), iPSCs and original fibroblasts with reference to previously deposited data of human naïve-like or primed-state ESCs (Chan et al., 2013). Hierarchical clustering analysis using the expression of major pluripotency/ectoderm-related genes indicated that the iNSLCs harbored a unique gene expression property distinct from that of both naïve-like and primed-state PSCs (as shown below, Log<sub>2</sub>FC scaling).

Differentiated from hiNSLCs EP-B



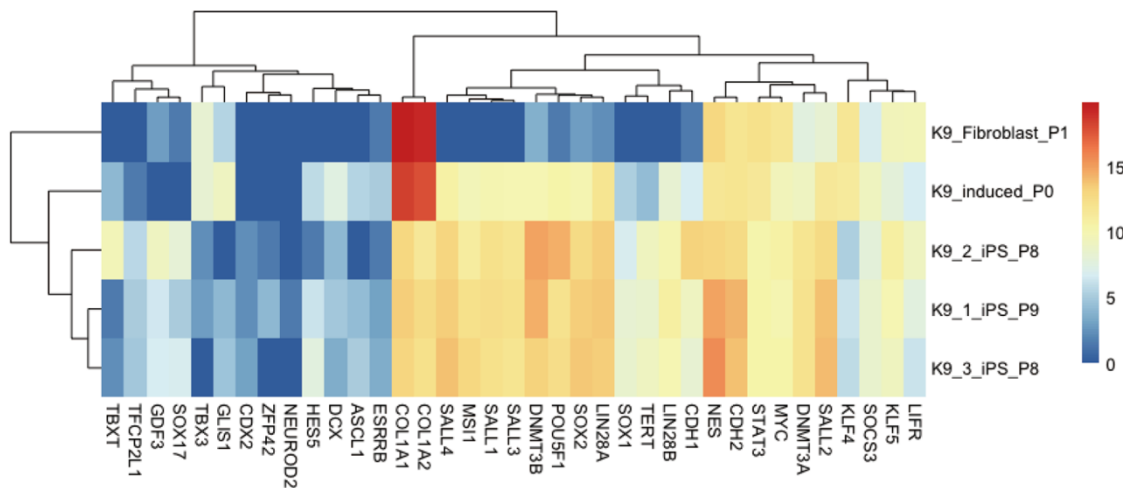
Based on these findings, we speculated that in our method, somatic fibroblasts from various mammalian species are likely to be reprogrammed to pluripotency via a route that passes through an NSC-like state.

**Note S6. Transcriptomic analysis of canine fibroblasts, iNSLCs and iPSCs (related to Figure 6).**

As shown on the right, by PCA using mRNA-seq data, we found that the primary colony-forming cells such as putative canine iNSLCs showed a clearly distinct profile of gene expression from the K9 iPSC #1–3 and original fibroblasts.

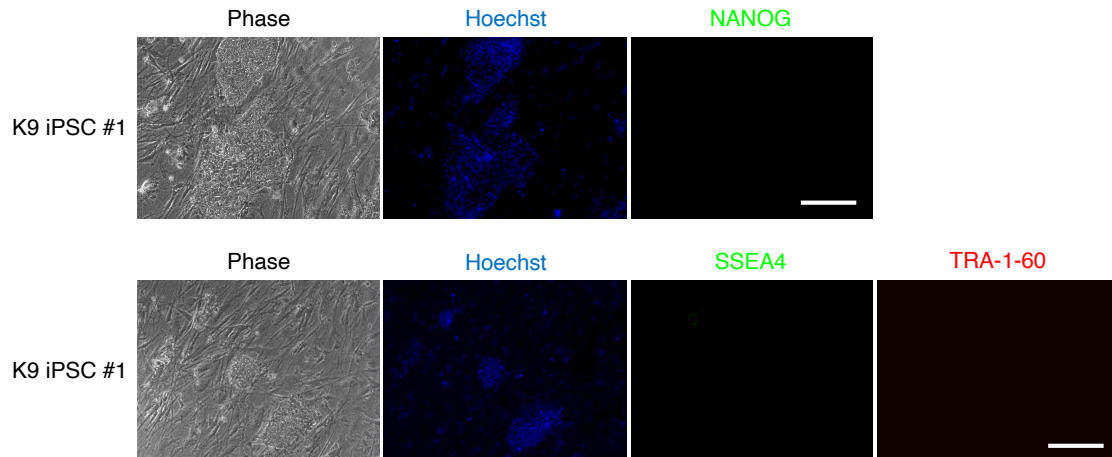


In addition, the iNSLCs showed enriched expression of some NSC/neuroblast markers such as *ASCL1* and *DCX*, while the iPSCs showed strong expression of major PSC markers including *POU5F1* (*OCT4*), *DNMT3A*, *DNMT3B* and *LIN28A* (*LIN28*), as shown below (Log<sub>2</sub>FC scaling).



**Note S7. Culture conditions for enhancement of PSC marker expression in ciPSCs (related to Figure 6).**

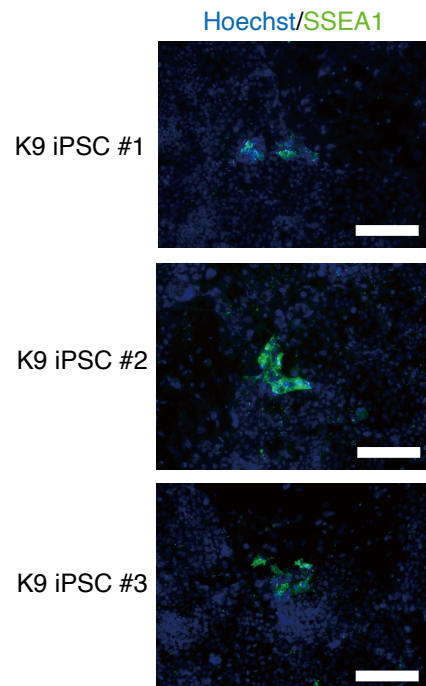
In the culture condition using ESM, canine iPSCs stained weakly or negatively for NANOG, SSEA4 and TRA-1-60 (as shown below, scale bars = 100  $\mu$ m).



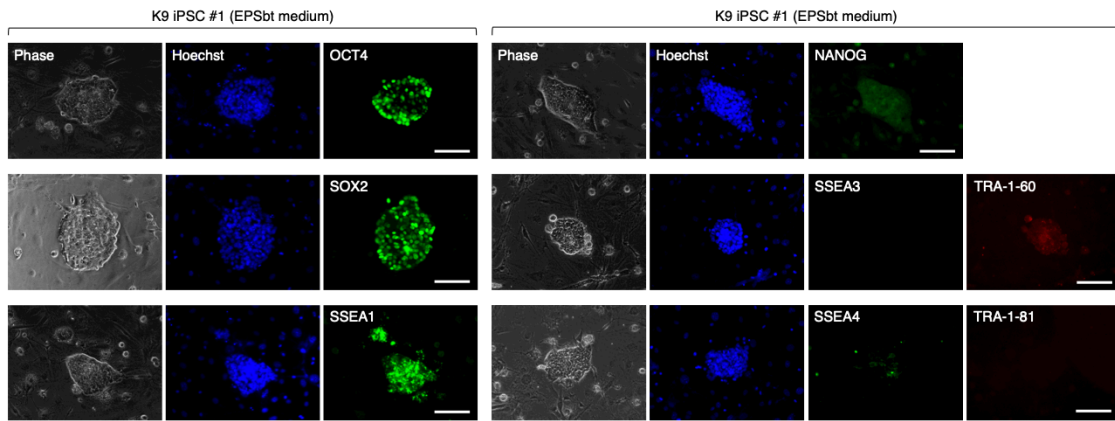
Among the PSC-related surface markers, only SSEA1 was positive for a small portion (~ 1%) of the canine iPSCs (as shown on the right, scale bars = 100  $\mu$ m), while SSEA3, SSEA4, TRA-1-60 and TRA-1-81 were negative (data not shown).

To explore culture conditions which could enhance PSC marker expression in the ciPSCs, we tested a condition recently reported for the culture of expanded pluripotent stem cells (EPSCs) in human and porcine cells (Gao et al., 2019), since it has been reported that the EPSC culture condition enabled the derivation of transgene-independent porcine iPSCs with robust PSC marker expression for the first time (Du et al., 2015). Although our initial attempts were

not successful because of the slow cell growth of ciPSCs in the original EPSC medium (data not shown), we discovered that the supplementation of bFGF (10 ng/ml) and TGF- $\beta$ 1 (10 ng/ml) in the EPSC medium, named EPSbt mem hereon, enabled the expansion of ciPSCs. As shown below (scale bars = 100  $\mu$ m), by immunocytochemistry, we found that canine iPSCs (K9 iPSC #1) became strongly positive for OCT4, SOX2 and also SSEA1, whose expression was reported in several studies using canine ESC-like cells (Hatoya et

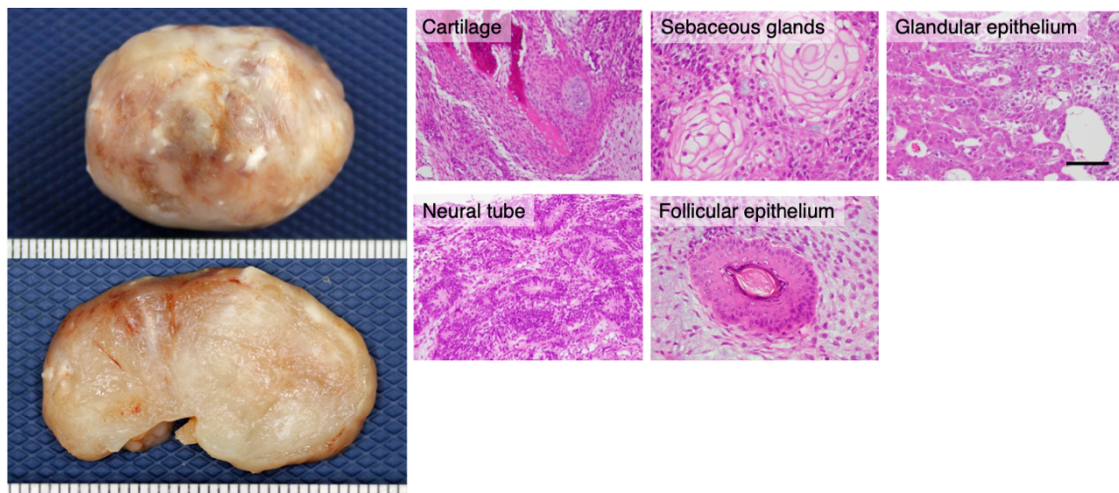


al., 2006; Schneider et al., 2007) and ciPSCs (Tsukamoto et al., 2018). Also, the iPSCs in EPSbt mem were weakly positive for NANOG and TRA-1-60, but still negative for SSEA3 and TRA-1-81.



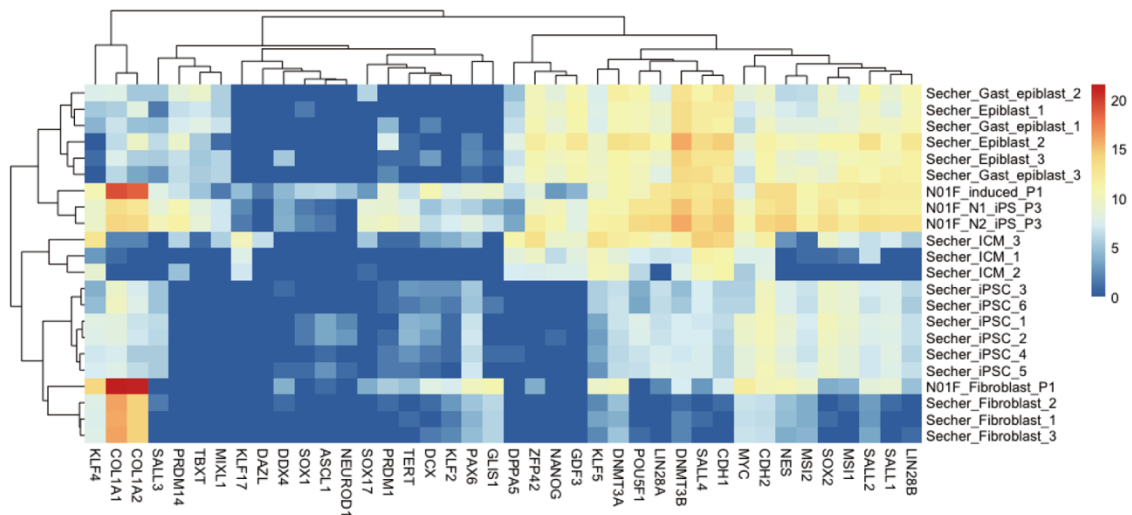
**Note S8. Assessment of the *in vivo* three-germ-layer differentiation potential of ciPSCs through teratoma formation.**

As shown below right (scale bar = 100  $\mu$ m), the *in vivo* three-germ-layer differentiation potential of canine iPSCs (K9 iPSC #1) was assessed by teratoma formation (a macroscopic image of the teratoma is shown below left) in NOD/SCID mice. As a result, the ciPSC differentiated into ectoderm (neural tube and sebaceous glands), mesoderm (cartilage and follicular epithelium) and endoderm (glandular epithelium).



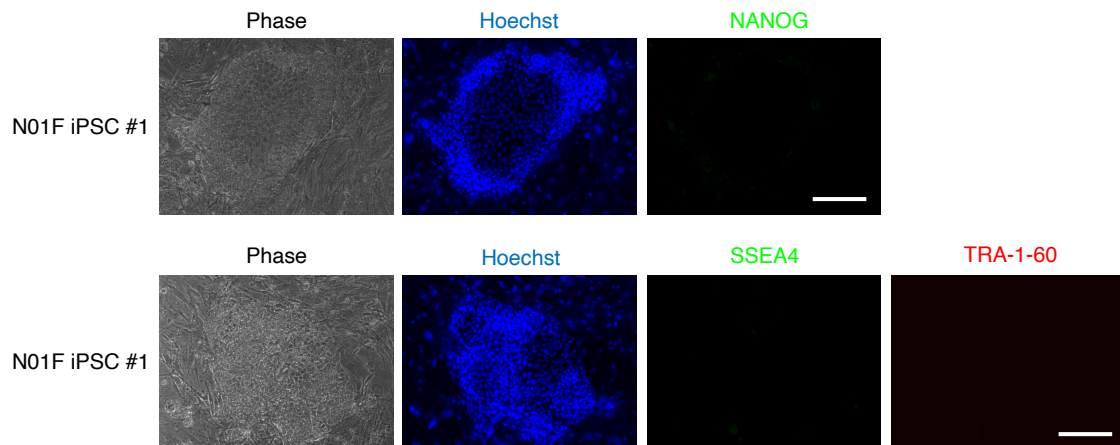
**Note S9. Transcriptomic analysis of porcine fibroblasts, iNSLCs and iPSCs (related to Figure 7).**

We also performed mRNA-seq analysis for dissecting the gene expression profiles of the porcine cells, using deposited data of piPSCs and early embryos from a previous study (Secher et al., 2017). By hierarchical clustering analysis using the expression of major pluripotency/ectoderm/fibroblast-related genes, N01F iPSC #1–2 (N01F N1–2 iP) were closely clustered with epiblasts and gastrulation epiblasts, which may reflect their primed-state pluripotency (as shown below, Log<sub>2</sub>FC scaling). We note that, distinct from marmoset and canine cells, the difference in gene expression property between cells during induction in NSM (putative iNSLCs; N01F\_induced\_P1) and piPSCs were comparatively subtle, while the putative iNSLCs showed enhanced expression of multiple ectodermal markers, including *SOX1*, *ASCL1*, *NEUROD1*, *DCX* and *PAX6*.

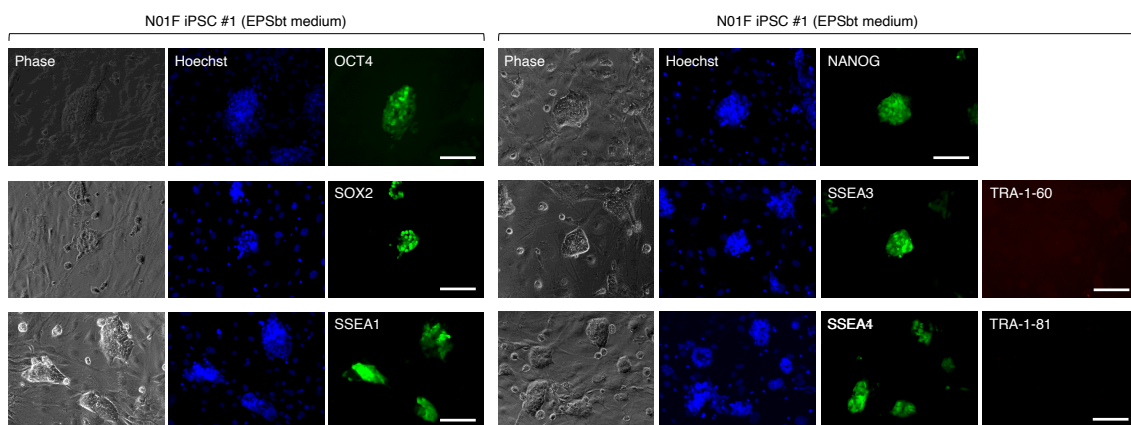


**Note S10. Culture conditions for enhancement of PSC marker expression in piPSCs (related to Figure 7).**

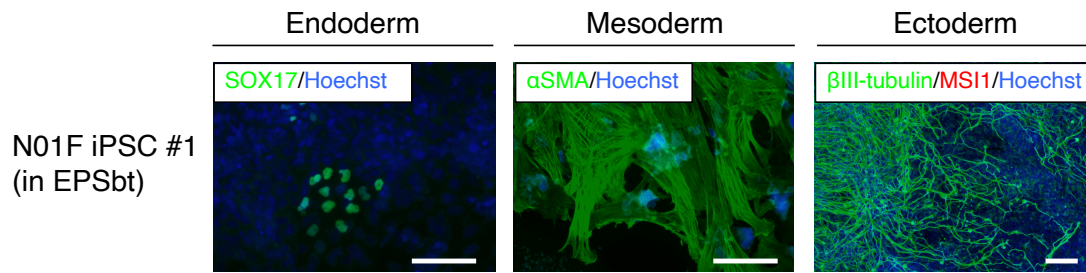
AP staining and immunocytochemical analyses showed that the piPSCs (N01F iPSC #1) strongly expressed AP, OCT4 and SOX2 (Figure 7C–E), while these cells were negative for NANOG, SSEA4 and TRA-1-60, as shown below (scale bars = 100  $\mu$ m).



To enhance PSC marker expression of the piPSCs, we also tested the EPSbt mem for culturing the piPSCs. As shown below (scale bars = 100  $\mu$ m), immunocytochemical analysis revealed that porcine iPSCs (N01F iPSC #1) became strongly positive for OCT4, SOX2, SSEA1, NANOG, SSEA3 and SSEA4, while still negative for TRA-1-60 and TRA-1-81.



In addition, these cells retained the three-germ layer differentiation capacity by EB formation as shown below (scale bars = 100  $\mu$ m).



**Note S11. Two possible mechanisms of transgene-free iPSC derivation from fibroblasts through an NSC-like state (related to the Discussion section in the main manuscript).**

First, when using chemical inhibitors, it has been suggested that the derivation of NSC-like cells from fibroblasts is more efficient than the direct derivation of iPSCs, which favor transgene expression over chemical induction for their generation. For instance, Lu *et al.* reported the derivation of neural progenitors from fibroblasts of humans and macaque monkeys using a medium containing N2/B27 supplements and LIF/CHIR/SB431542 (a TGF- $\beta$  inhibitor), which are similar to the components of NSM, as well as Sendai virus vectors harboring *OCT4*, *SOX2*, *KLF4* and *C-MYC* (Lu et al., 2013). The existence of this phenomenon was also supported by similar studies using somatic fibroblasts of mice (Kim et al., 2011) and humans (Wang et al., 2013), which emphasizes a sharp difference from the conventional reprogramming route of hiPSCs through an incipient mesendodermal-like state (Takahashi et al., 2014). Although Nakajima-Koyama *et al.* reported the reprogramming of murine adult astrocytes toward a pluripotent state through an NSC-like state (Nakajima-Koyama et al., 2015), and the several studies implied the existence of an NSC-mediated reprogramming route (Kim et al., 2011; Lu et al., 2013; Wang et al., 2013), substantial demonstration of the somatic cell-to-NSC-to-PSC reprogramming phenomenon has not been performed for any non-ectodermal cells including somatic fibroblasts in any mammalian species.

Second, NSCs have a higher potential to be reprogrammed into iPSCs than fibroblasts. Although there is a variation of results among reports, Di Stefano *et al.* showed that NSCs were reprogrammed into iPSCs more efficiently than embryonic fibroblasts in mice (Di Stefano et al., 2009). Additionally, for reprogramming NSCs toward pluripotency, only *OCT4* overexpression was required in both mouse (Kim et al., 2009b) and human NSCs (Kim et al., 2009a). Taken together, it is plausible that the

iNSLCs in our study, which continued to express exogenous transgenes and were transcriptionally similar to NSCs, possess a high potential to be converted into iPSCs.

**Note S12. Significance of the derivation of transgene-free ciPSCs and piPSCs in this study (related to the Discussion section in the main manuscript).**

Earlier studies on the generation of ciPSCs used transgene-integrating viral vectors, and reported the dependency on transgene expression for the maintenance of the pluripotent state (Lee et al., 2011; Luo et al., 2011; Nishimura et al., 2017; Shimada et al., 2010). More recently, two studies demonstrated the generation of transgene-free ciPSCs using Sendai virus vectors (Chow et al., 2017; Tsukamoto et al., 2018). However, to our knowledge, the present study is the first report to have utilized non-viral methods for deriving transgene-free ciPSCs.

Although significant efforts have been made to derive transgene-free piPSCs (Cong et al., 2019; Ogorevc et al., 2016), multiple studies reported the difficulty in deriving transgene-free iPSCs from porcine fibroblasts, even with intensive drug selection (Du et al., 2015; Wu et al., 2009). Importantly, although the pig is the only non-rodent mammalian species reported to have achieved successful germline-transmitting chimera formation from iPSCs through blastocyst injection (West et al., 2011), residual expression of transgenes affected the developmental potential of the iPSCs, which resulted in the stillborn or premature death of the offspring (West et al., 2011). More recently, Gao *et al.* successfully derived piPSCs using a PiggyBac-transposition-based Dox-inducible vector system and the EPSC medium. Unlike some earlier studies (Du et al., 2015; Esteban et al., 2009; Ezashi et al., 2009; Wu et al., 2009), piPSCs derived by Gao *et al.* retained pluripotency without Dox supplementation i.e. transgene expression (Gao et al., 2019). However, for the first time, this present study succeeded in the complete removal of the transgene sequences from the piPSCs.

## **Supplemental Figure Legends**

**Figure S1 (related to Figure 1). Derivation of primary colonies from marmoset fibroblasts using episomal vectors.**

(A) Representative bright-field (BF) and green-fluorescence (EGFP) images of E01F fibroblasts 4 days after transfection of the EP-A vector set. Scale bars = 100  $\mu$ m. (B) Representative images of E01F and E02M fibroblasts 30 days after transfection of the



EP-A vector set, which were cultured in ESM. No colony was derived. Scale bars = 200  $\mu\text{m}$ .

(C) Immunocytochemical staining of primary colonies derived from E01F fibroblasts in NSM using the SOX2 antibody. Hoechst was used for blue nuclear staining. Scale bars = 100  $\mu\text{m}$ .

(D) AP staining of primary colonies derived from embryonic E01F fibroblasts (EP-A and EP-B transfected) in NSM. Cells stained dark purple were AP-positive. Scale bars = 200  $\mu\text{m}$ .

(E) Immunocytochemical staining of primary colonies derived from E01F fibroblasts (EP-A and EP-B transfected) in NSM using primary antibodies of PSC markers such as TRA-1-60 and SSEA4. Scale bars = 100  $\mu\text{m}$ .

(F) Immunocytochemical staining of primary colonies derived from E01F fibroblasts (EP-B transfected) in NSM using MS11 and TRA-1-60 antibodies. Scale bars = 100  $\mu\text{m}$ .

**Figure S2 (related to Figures 2–3). Derivation and characterization of marmoset transgene-free iPSCs.**

(A) AP staining of twelve iPSC lines derived from adult marmosets (I5061F and CM421F). Scale bars = 500  $\mu\text{m}$ .

(B) Immunocytochemical staining of eight iPSC lines derived from adult marmosets using TRA-1-60 and SSEA4 antibodies. Scale bars = 100  $\mu\text{m}$ .

(C–H) qPCR analysis of iPSCs using specific primers for endogenous (endo) PSC marker genes (*OCT4*, *NANOG*, *SOX2*, *KLF4*, *ZFP42*, *LIN28*, *DPPA5* and *TERT*) ( $n = 3$ , independent experiments).

**Figure S3 (related to Figures 2–3). DNA analysis.**

(A–D) Genomic PCR analysis of iPSCs derived from embryonic (A) and adult marmosets (B) for the detection of residual episomal vectors using specific primers for the OriP sequence (Yu et al., 2009). Primers for the endogenous marmoset *OCT4* locus were used as an internal control. PCR analyses shown in (C) and (D) were performed to independently amplify OriP and *OCT4* sequences, which was simultaneously performed in (A).

(E) Assessment of the OriP detection sensitivity of PCR using pCE-hUL, supplemented 100 pg, 10 pg, 1 pg, or 0.1 pg in each PCR solution. Approximately, 0.1 pg of pCE-hUL

(11235 bp) is  $8.13 \times 10^3$  copies. For the genomic PCR analysis, we used 100 ng of genomic DNA in each PCR solution, which is approximately equivalent to  $1.5 \times 10^4$  copies of marmoset genomic DNA (approximately 30 Mbp).

(F) Schematic of episomal vectors used in this study (vector sets were shown in Figure 1A) and the binding sites of the primers (black arrows) for each episomal vector. Each primer set was abbreviated as following in Figure S3D–F: OC, SK, UL, MP, KN and KG.

(G) The primers specific for each vector were validated by PCR using the genomic DNA of E01F fibroblasts (WT; negative control) and EP-B transfected E01F fibroblasts (Day4; positive control)

(H) Genomic PCR analysis for iPSCs and iNSLCs derived from embryonic marmosets using specific primers for each episomal vector. Genomic DNA extracted from two embryo-derived OriP(–) iPSCs (E01F A-2-2 and E02M B-0-7), two embryo-derived OriP(+) iPSCs (E01F A-2-4 and E02M B-0-11), two embryo-derived OriP(+) iNSLCs (E01F A-2 and E02M B-4), and two adult-derived OriP(–) iPSCs (I5061F B-3-3 and CM421F B-0-12) were used.

(I) Genomic PCR analysis for iNSLCs that were competent for primed conversion (E01F A-2 iNSLC P1 and I5061F B-3 iNSLC P1).

#### **Figure S4 (related to Figure 2 and 3). Karyotyping analysis of marmoset iPSCs.**

(A) Chromosome counting of six marmoset iPSC lines (E01F A-2-2, E01F A-2-6, E01F A-2-7, E02M B-0-7, I5061F B-3-3 and CM421F B-0-4) by G-banding. Fifty cells were used in each cell line (except I5061F B-3-3, which we used forty-three cells). Gray bars show euploid ( $2n = 46$ ) cells. Numerics on bars show the number of counted cells (in fifty cells) harboring each number of chromosomes.

(B) Q-banding-based karyotyping of euploid cells from six marmoset iPSC lines (E01F A-2-2, E01F A-2-6, E01F A-2-7, E02M B-0-7, I5061F B-3-3 and CM421F B-0-4).

(C) Sex of the marmoset ESCs and iPSCs used in this study was validated by PCR using primers specific for the marmoset *GAPDH* (control) and *SRY* loci. Only DSY127 and E02M B-0-7 showed *SRY*-positive PCR bands. High resolution images of karyotyping are shown in Supplementary Data 3.

#### **Figure S5. PGCLC induction from marmoset PSCs.**

(A) Graphical schematic of reporter constructs (*BLIMP1-Venus* and *VASA-tdTomato*) for

marmoset iPSCs. Using *Cas9/gRNA* and *BLIMP1-Venus* targeting vector as described previously (Yoshimatsu et al., 2020; Yoshimatsu et al., 2019c), the endogenous *BLIMP1* locus was targeted (top). Following hygromycin selection, and subsequent G418 and ganciclovir selection, the resultant iPSCs harbored the *BLIMP1-Venus* knock-in alleles and *VASA-tdTomato* transgene (bottom). Black and gray boxes indicate endogenous exons (coding sequence and UTR) of *BLIMP1*. ITR, *Piggybac* inverted terminal repeats; PGK, Mouse *phosphoglycerate kinase 1* promoter; Hyg  $\Delta$ TK (HygTK), *hygromycin resistance gene* fused to the N-term-truncated *thymidine kinase*; pA, polyadenylation signal sequence; Neo; *neomycin resistance gene*. Instead of neomycin, G418 (an analogue of neomycin) was used for the selection experiment.

(B) Genotyping PCR of *BLIMP1* targeted iPSCs. Eight iPSC clones after hygromycin selection were genotyped for the detection of *BLIMP1-Venus-HygTK* knock-in (top). The homozygous knock-in clone #8 (named BV8) was used for transfection of a *HyPBase* expression vector and *VASA-tdTomato* reporter. Following G418 and ganciclovir selection, the excision of the PGK-HygTK cassette was confirmed by PCR (bottom). The clone #1 (named BV8VT1) was used for further induction experiments.

(C) Timetable of PGCLC induction (from Day 0 ~ 10). See Supplementary Methods for the detail.

(D) Transgene vectors of the dexamethasone/doxycycline-inducible *SOX17/BLIMP1* overexpression system. CAG, CAG promoter; rtTAM2, *reverse tetracycline-controlled transactivator M2*; IRES, internal ribosome entry site from *encephalomyocarditis virus*; TRE, tetracycline-responsive promoter element; Puro  $\Delta$ TK, *puromycin resistance gene* fused to the N-term-truncated *thymidine kinase*; HS4, chicken  $\beta$ -globin insulator.

(E) Representative phase-contrast/fluorescence images of Day9 aggregates from marmoset ESCs (No.40 BVSCVT2 (Yoshimatsu et al., 2019c) and DSY127 BV8VT1 (Yoshimatsu et al., 2020)) and E01F A-2-2 BV8VT1 iPSCs. Scale bars, 100  $\mu$ m.

(F) FACS analysis of *BLIMP1-Venus* fluorescence in single-cell-dissociated Day10 aggregates from marmoset ESCs and iPSCs. Venus fluorescence was detected by the FITC filter. 7-AAD (APC filter) was used for the removal of dead cells.

(G) PCA of marmoset ESCs and iPSCs (PSCs; green dots) and PGCLCs (Day10 *BLIMP1-Venus*-positive cells; red dots) and a whole testis from a 3-year-old marmoset (Adult\_Testis; a blue dot).

(H) Volcano plot of DEG analysis (PGCLC vs PSC samples).

(I) Heatmapping of pluripotency and germ cell lineage-related marker genes.

**Figure S6 (related to Figure 4). Characterization of marmoset iNSLCs.**

(A) qPCR analysis of early ectodermal markers (*SOX1* and *ZFP521*) in iNSLCs.

(B) qPCR analysis of early-mesodermal (*T*) and endodermal (*SOX17*) markers in iNSLCs.

(C–D) qPCR analysis of PSC markers (*OCT4*, *NANOG*, *SOX2*, *KLF4*) and NSC markers (*SOX1* and *PAX6*) in the iNSLCs at early passages (P1–2). For *OCT4* and *NANOG*, primers for both endogenous (endo) and exogenous (exo) sequences were used.

(E–F) Immunocytochemical staining of iNSLCs using primary antibodies of NSC (MS11, PAX6 and SOX2) and neuroblast (DCX) markers. Scale bars = 100  $\mu$ m.

(G) Timetable for the direct neurosphere formation assay.

(H) Differentiation efficiency of  $\beta$ III-tubulin-positive neurons ( $\beta$ III-tubulin(+)) from ESCs, iPSCs and iNSLCs.

(I) Representative images of  $\beta$ III-tubulin-positive neurons derived from the iNSLCs by the method shown in (A). Scale bars = 100  $\mu$ m.

(J–L) Immunocytochemical analysis of differentiated cells from the I5061F B-0 iNSLCs, using primary antibodies of  $\beta$ III-tubulin (neurons), GFAP (glial cells), Islet1 and ChAT (motor neurons), GalC (oligodendrocytes). Scale bars = 50  $\mu$ m.

**Figure S7. Assessment of the gene expression difference between iPSCs and iNSLCs (related to Figure 5).**

(A) Volcano plot of DEG analysis (iPSC vs iNSLC samples) using data from bulk mRNA-seq analysis. Significance was defined as fold change (FC) > 5 and  $p < 0.01$ . Genes that were significantly expressed in iPSCs are shown in warm colors. Genes that were significantly expressed in iNSLCs are shown in cold colors.

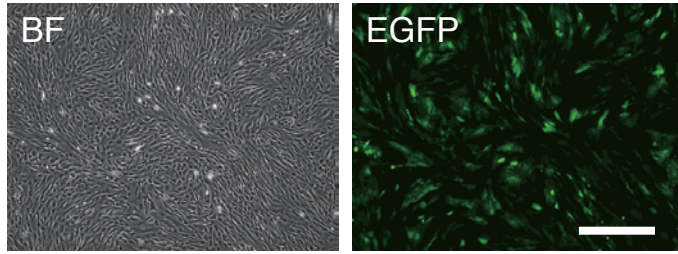
(B) Single-cell PCA of No.40 ESCs (n = 4; red dots), an E01F A-2-2 iPSC (n = 1; an orange dot), E01F A-2 iNSLCs at an early passage (P1; n = 65; black dots) and an E01F fibroblast (n = 1; a green dot) using RamDA-seq data.

(C) Box plots of *ASCL1*, *DCX*, *PAX6* and *NEUROG2* (genes significantly expressed in iNSLCs). Triangles show the expression levels in respective (single) cells.

(D) Box plots of *TDGF1*, *UTF1*, *EPCAM*, *ZFP42* and *DPPA2* (genes significantly expressed in iPSCs). Triangles show the expression levels in respective (single) cells.

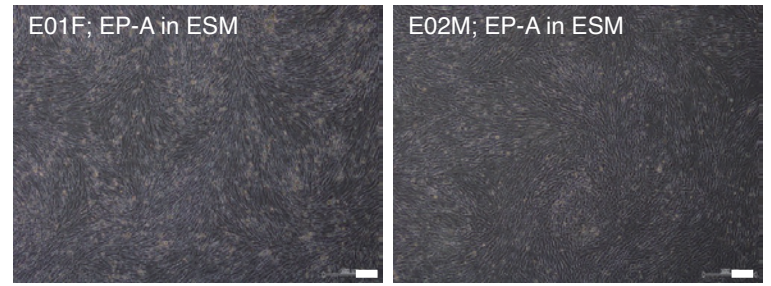
# Figure S1

## A E01F fibroblast (+EP-A) Day4

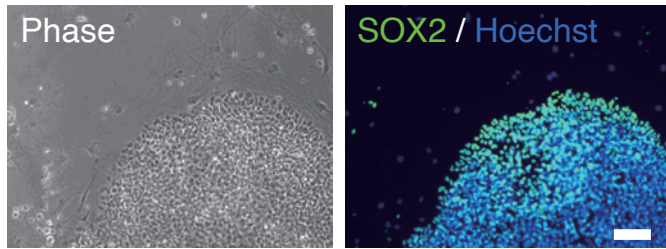


## B

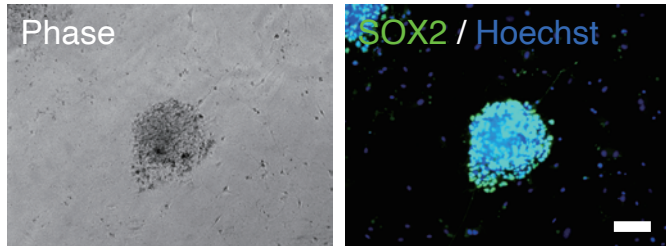
Day30



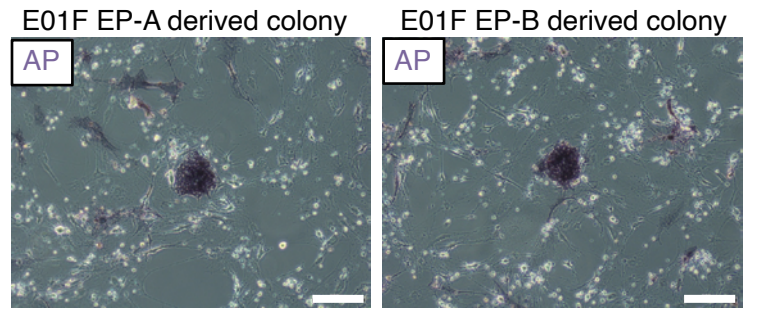
## C E01F EP-A derived colony



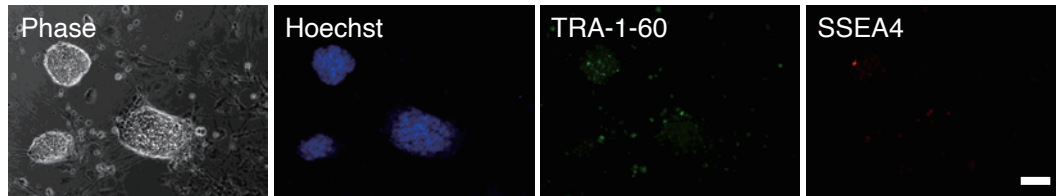
## E01F EP-B derived colony



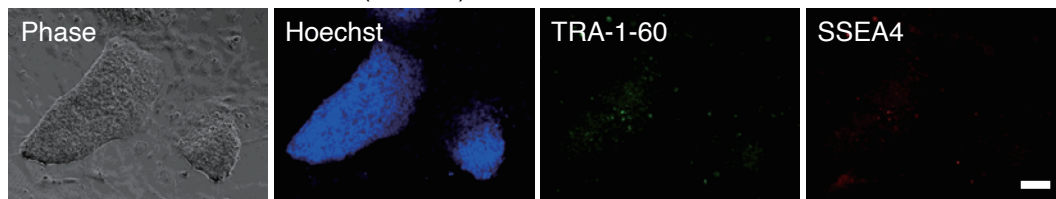
## D



## E E01F EP-A derived colonies (in NSM)



## E01F EP-B derived colonies (in NSM)



## F

## E01F EP-B derived colony

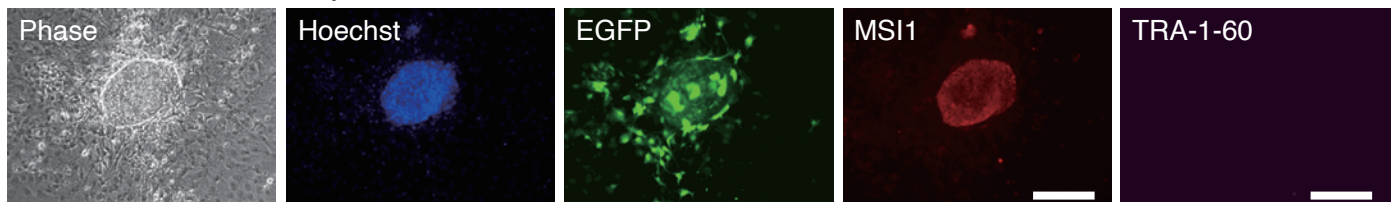
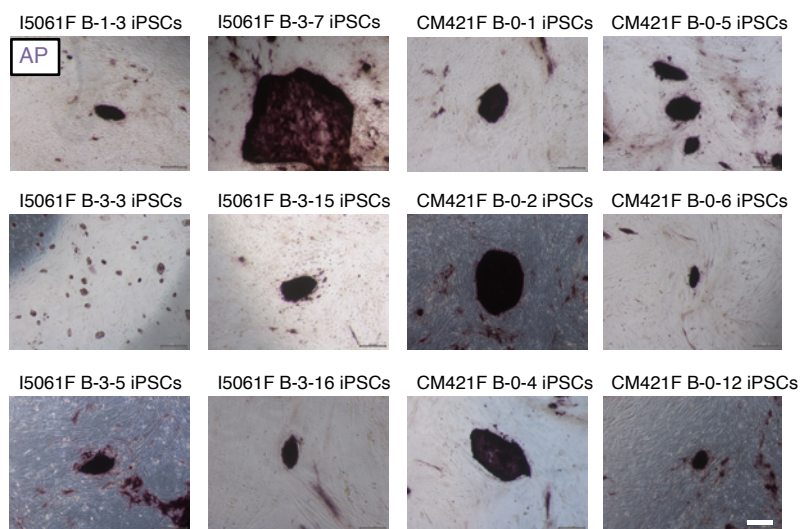
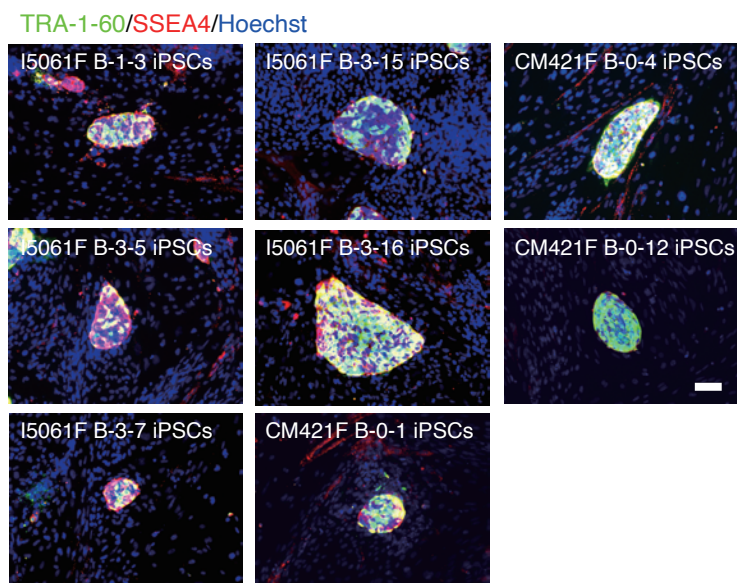


# Figure S2

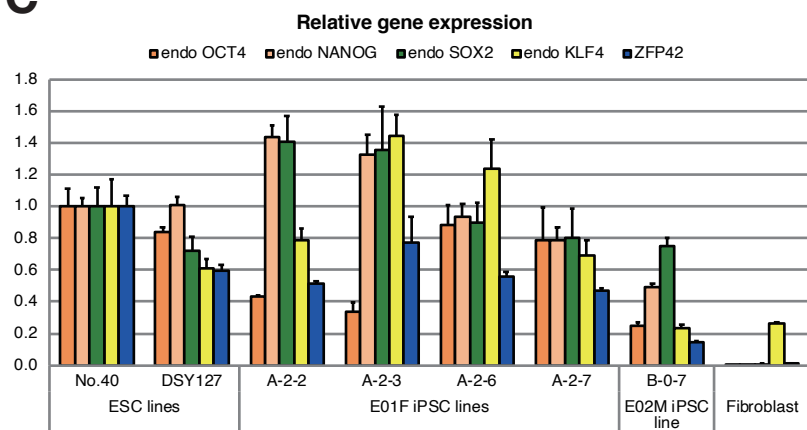
**A**



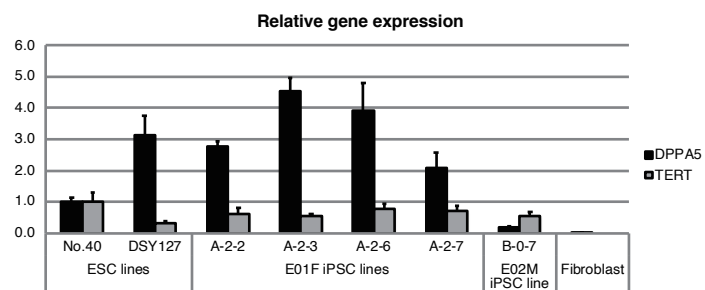
**B**



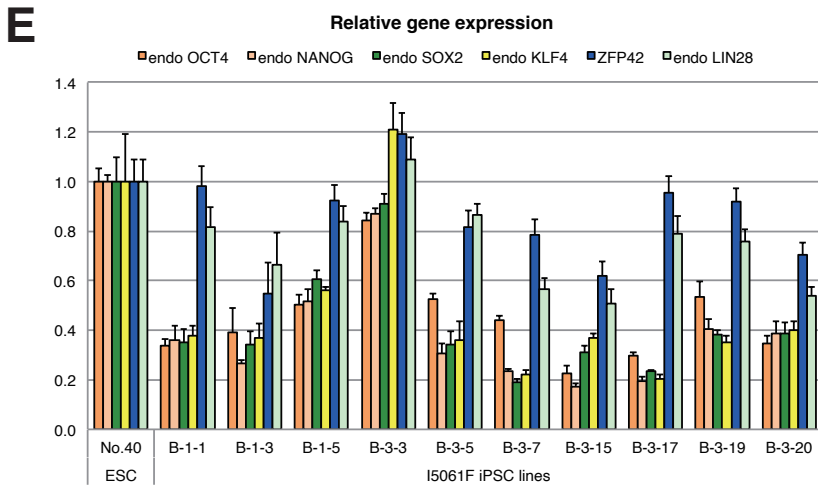
**C**



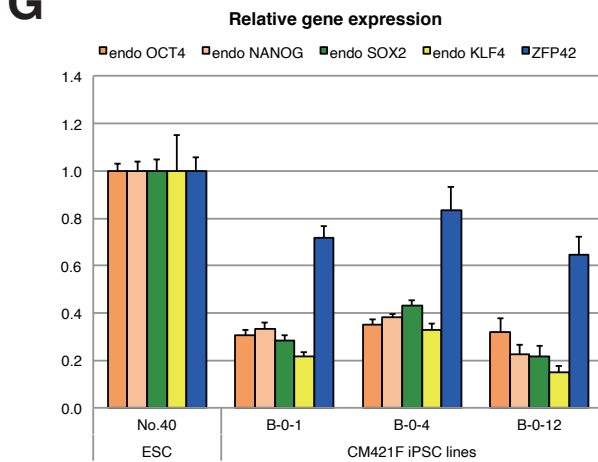
**D**



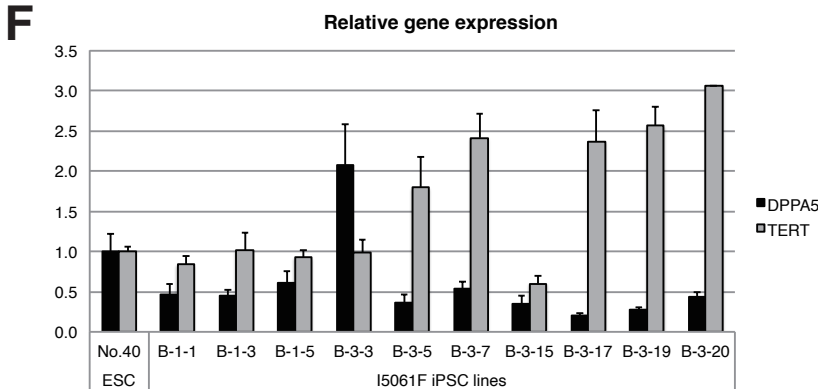
**E**



**G**



**F**



**H**

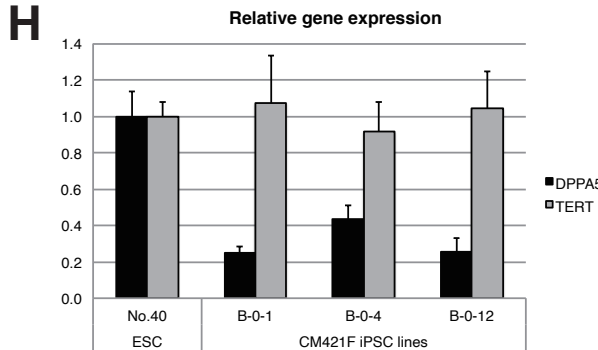


# Figure S3

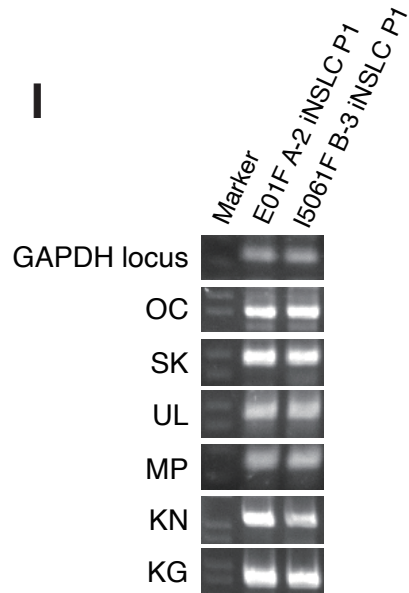
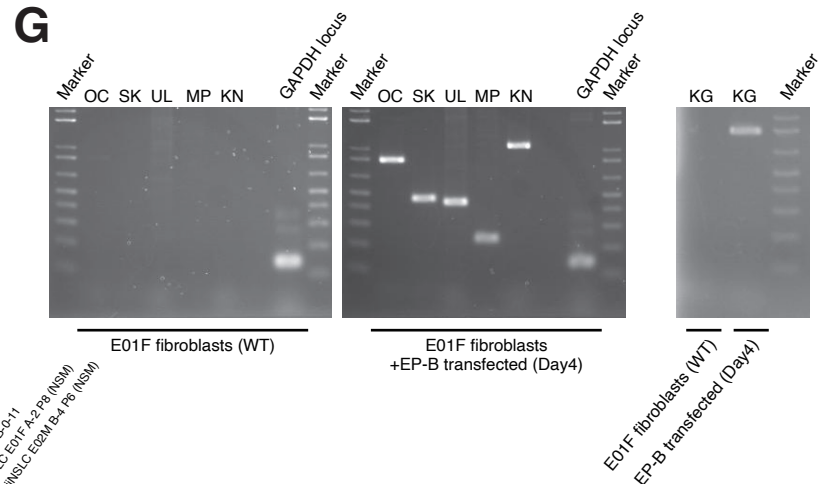
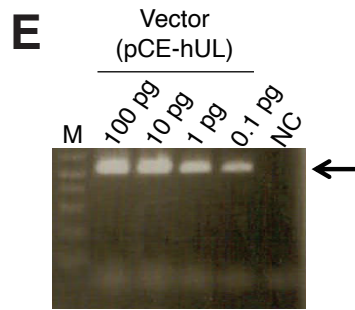
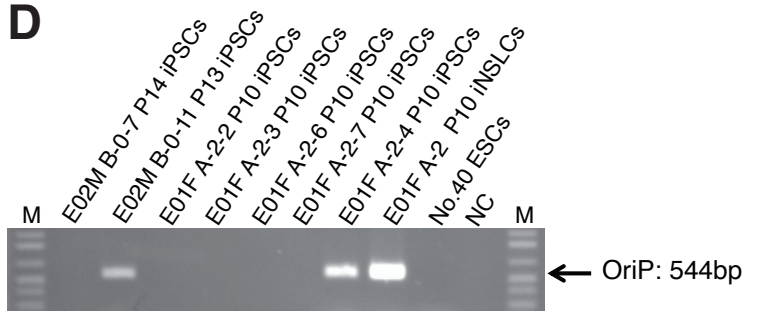
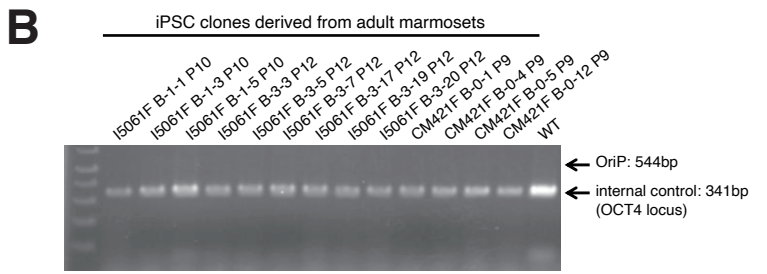
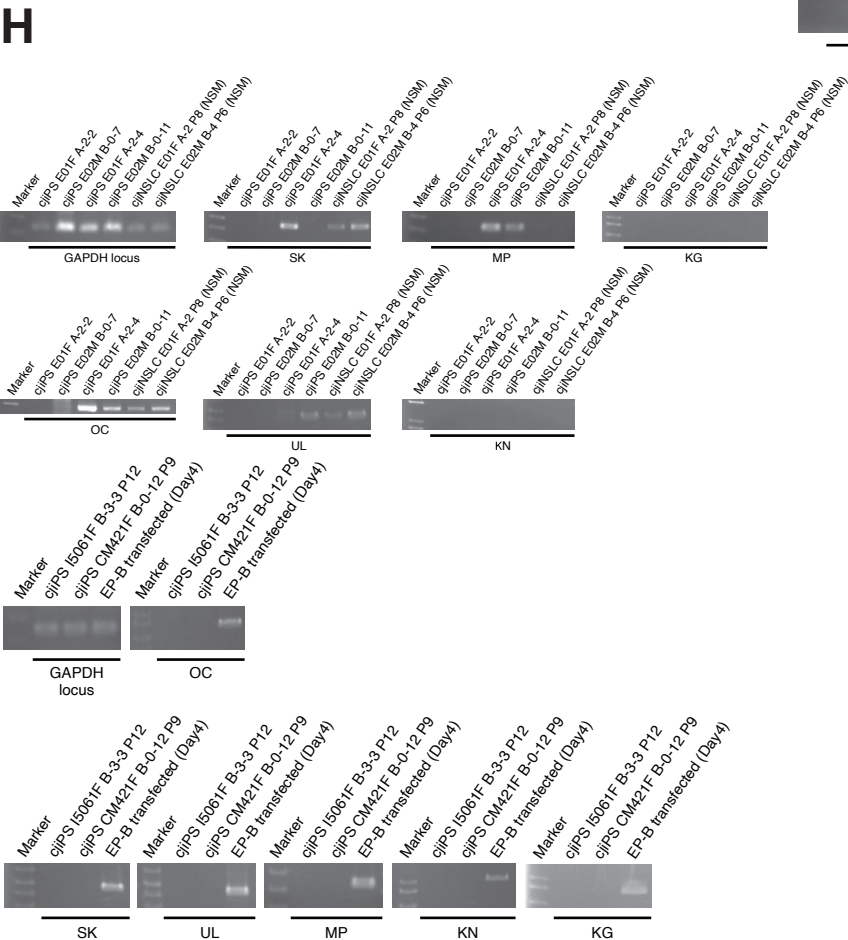
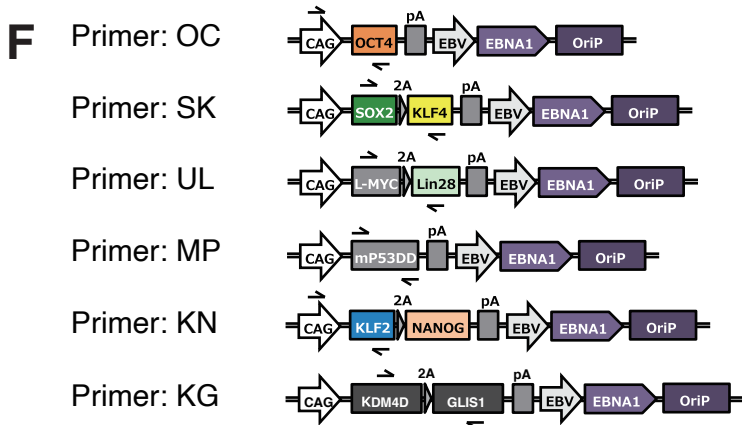
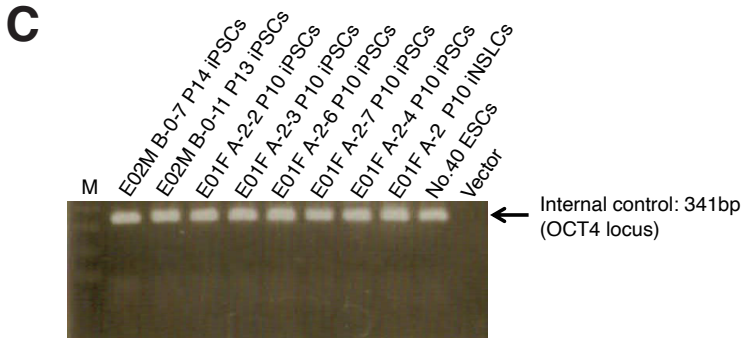
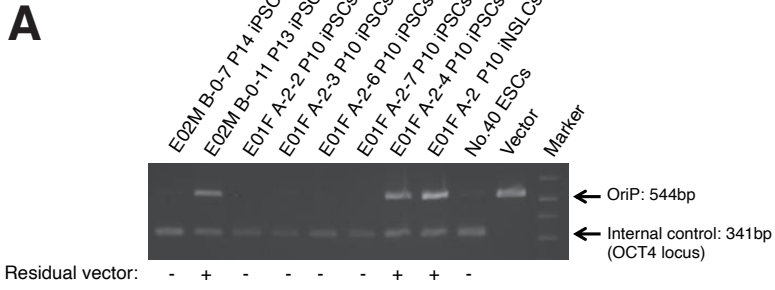
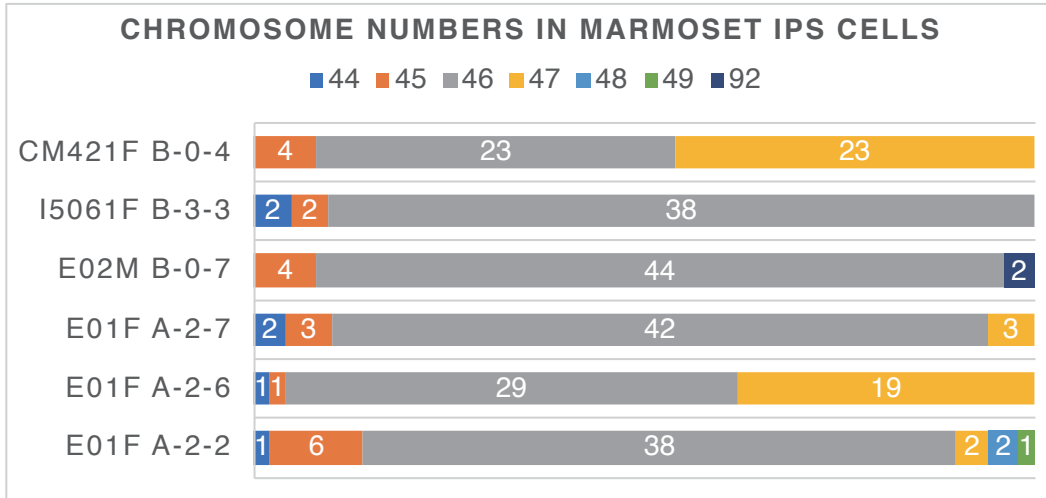
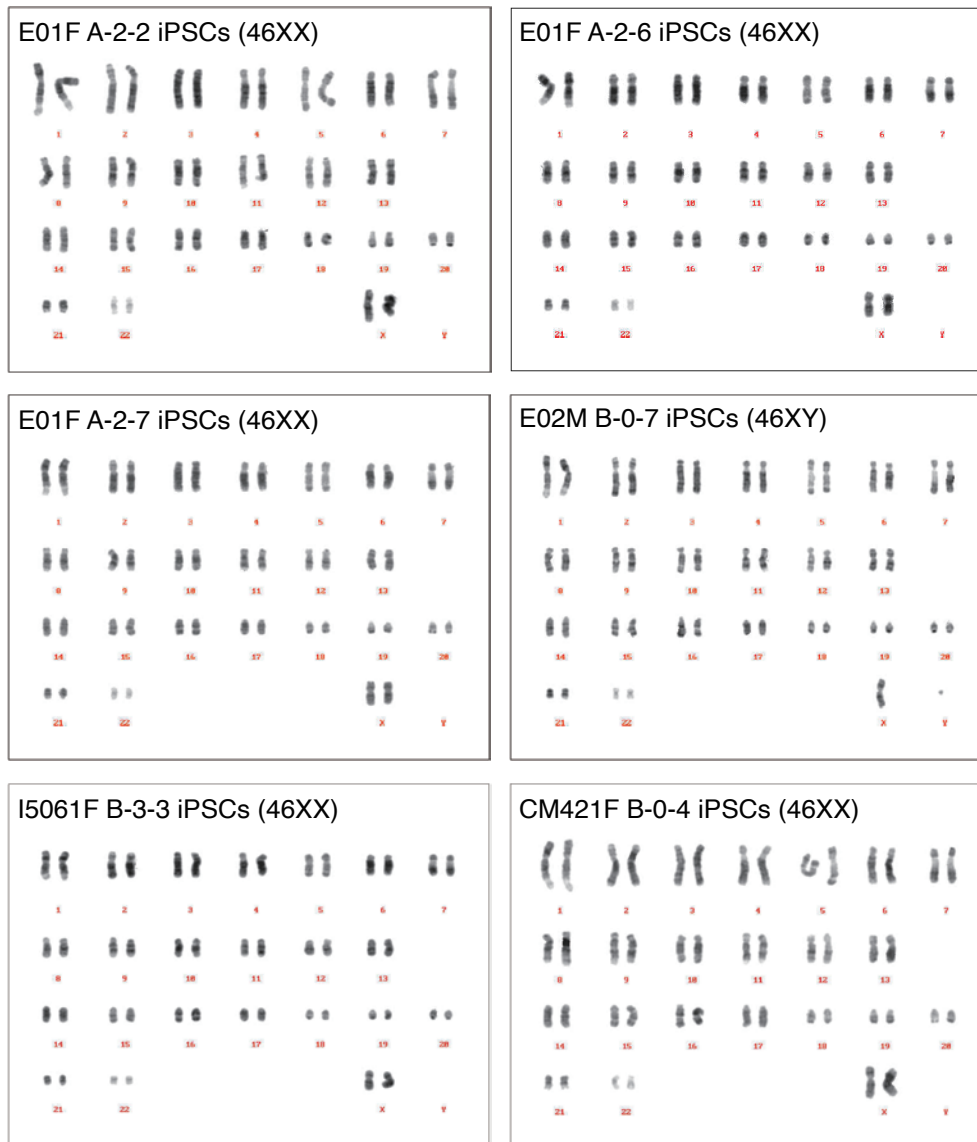


# Figure S4

**A**



**B**



**C**

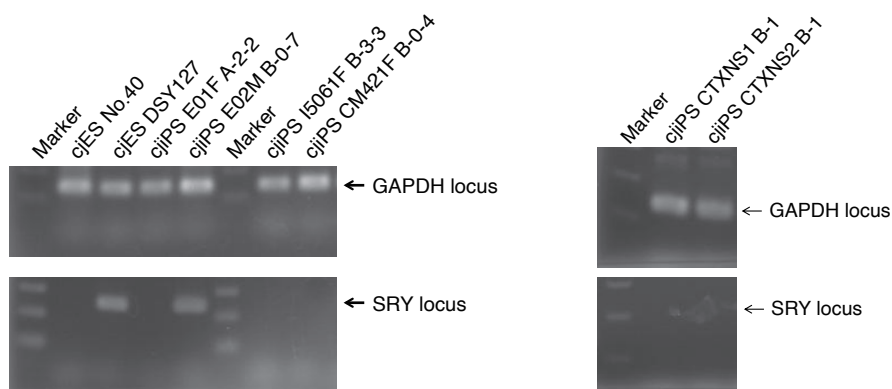




# Figure S5

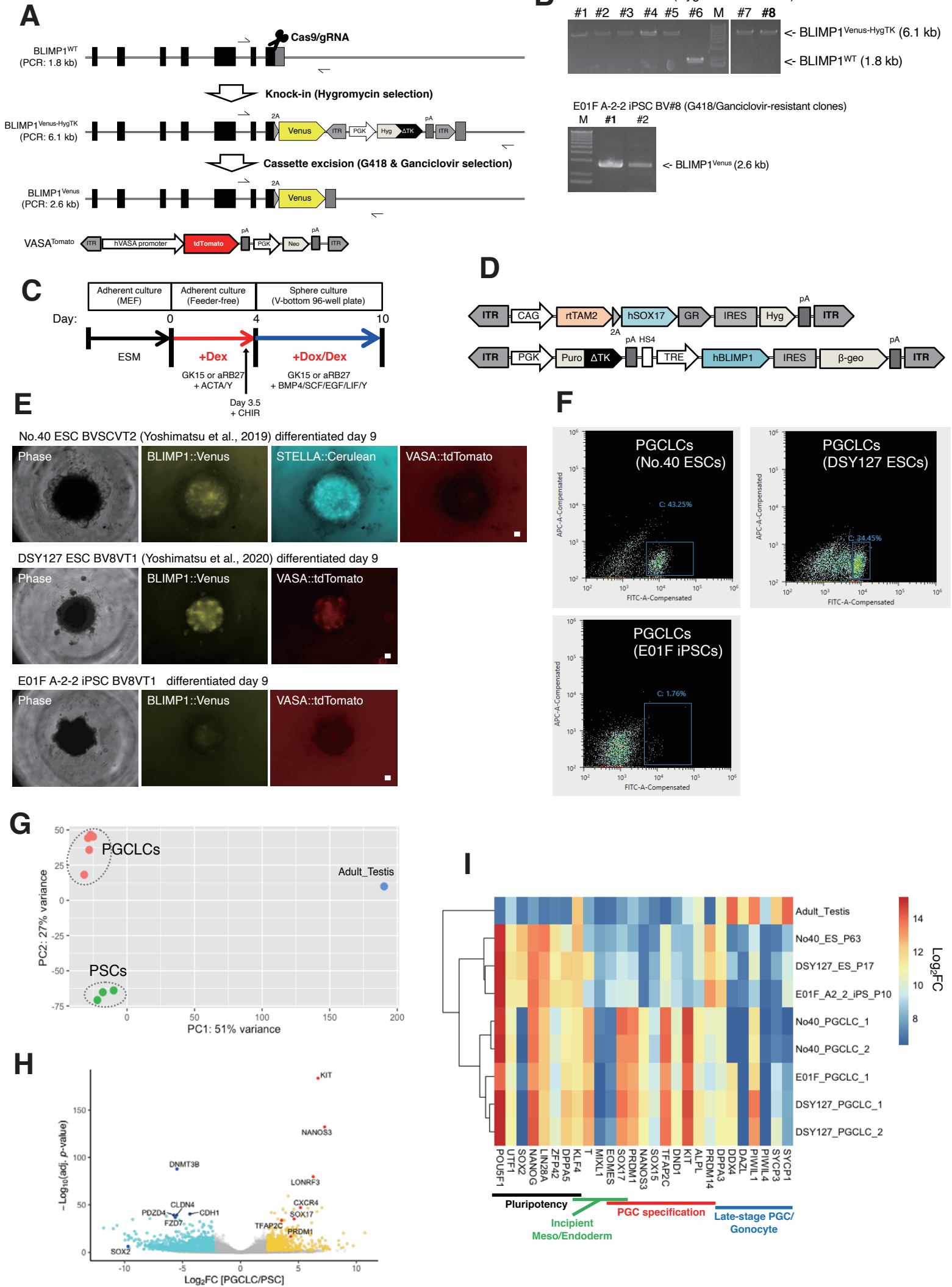


# Figure S6

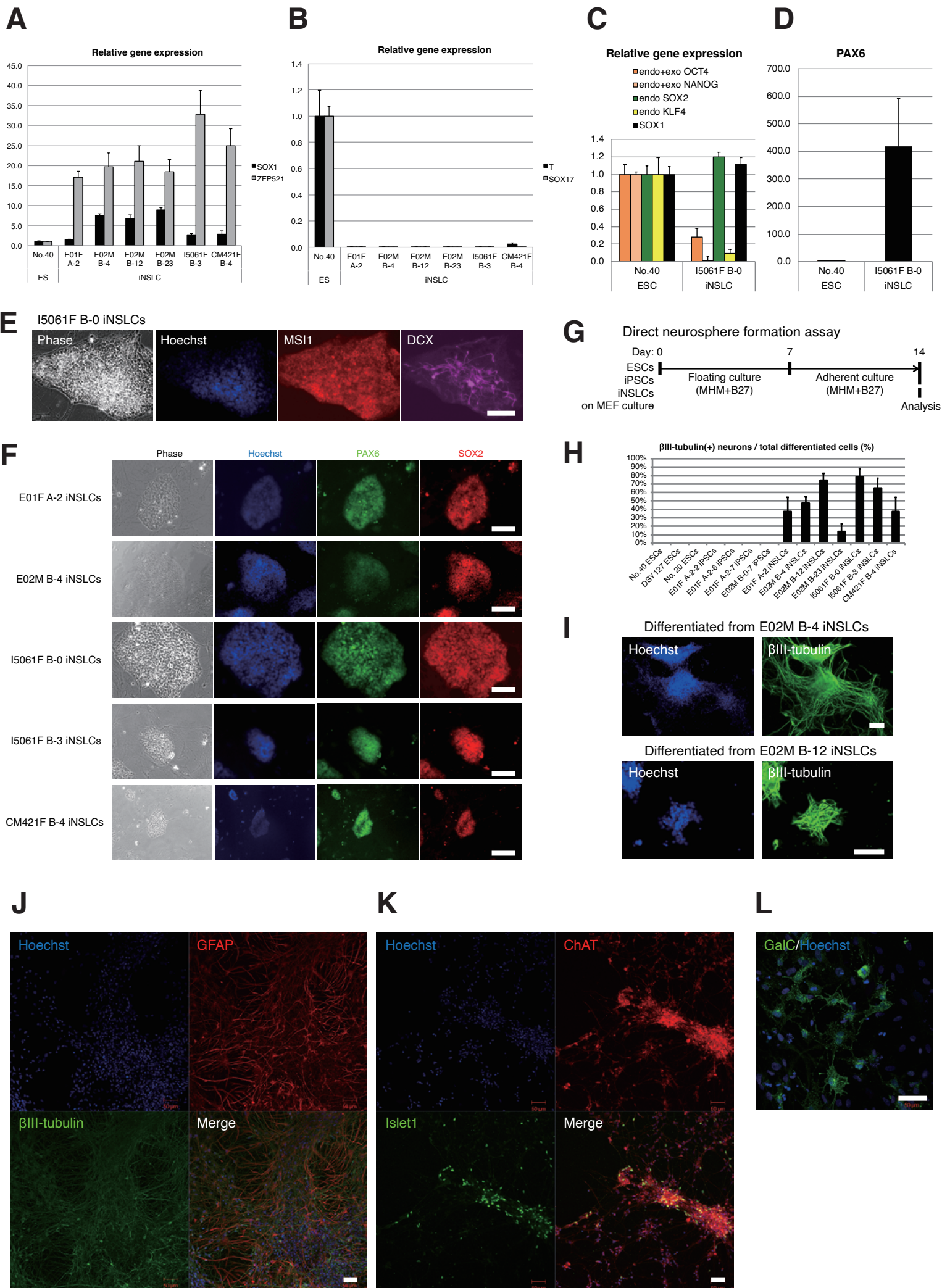
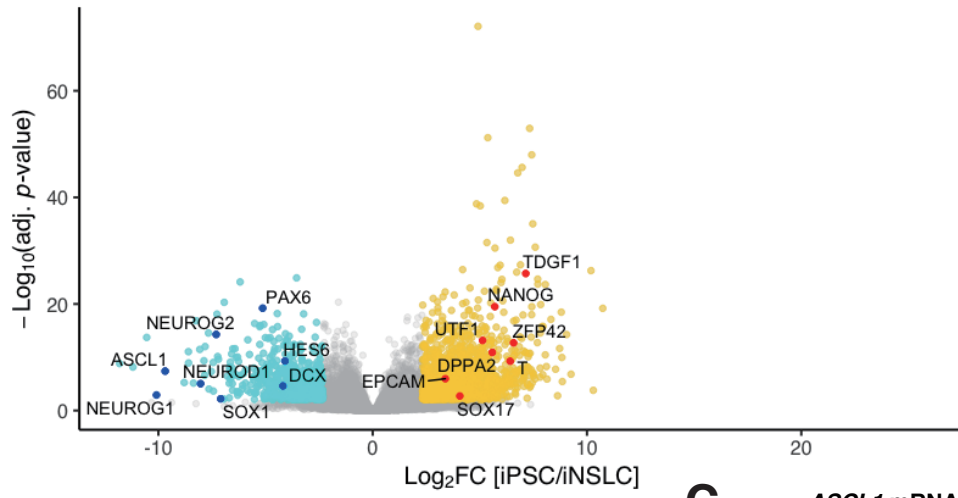
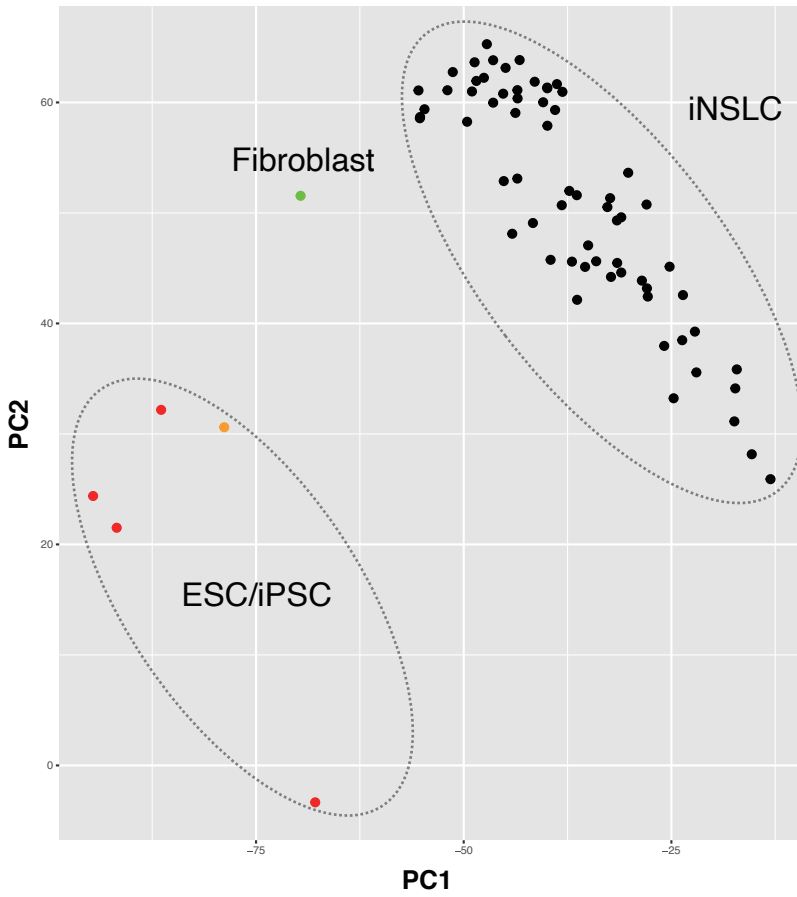


# Figure S7

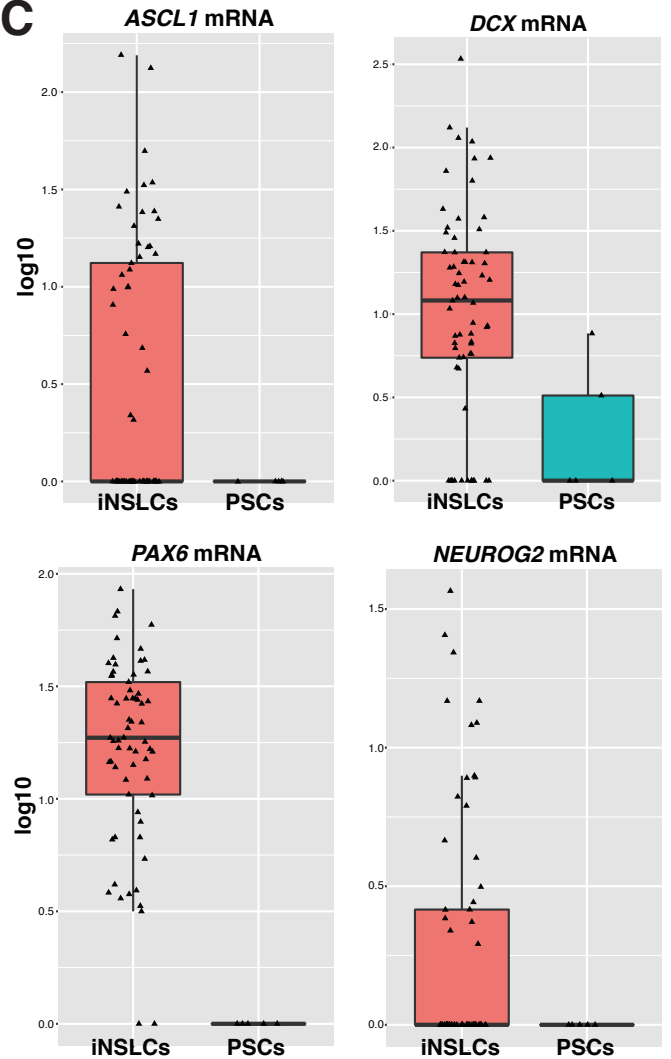
## A



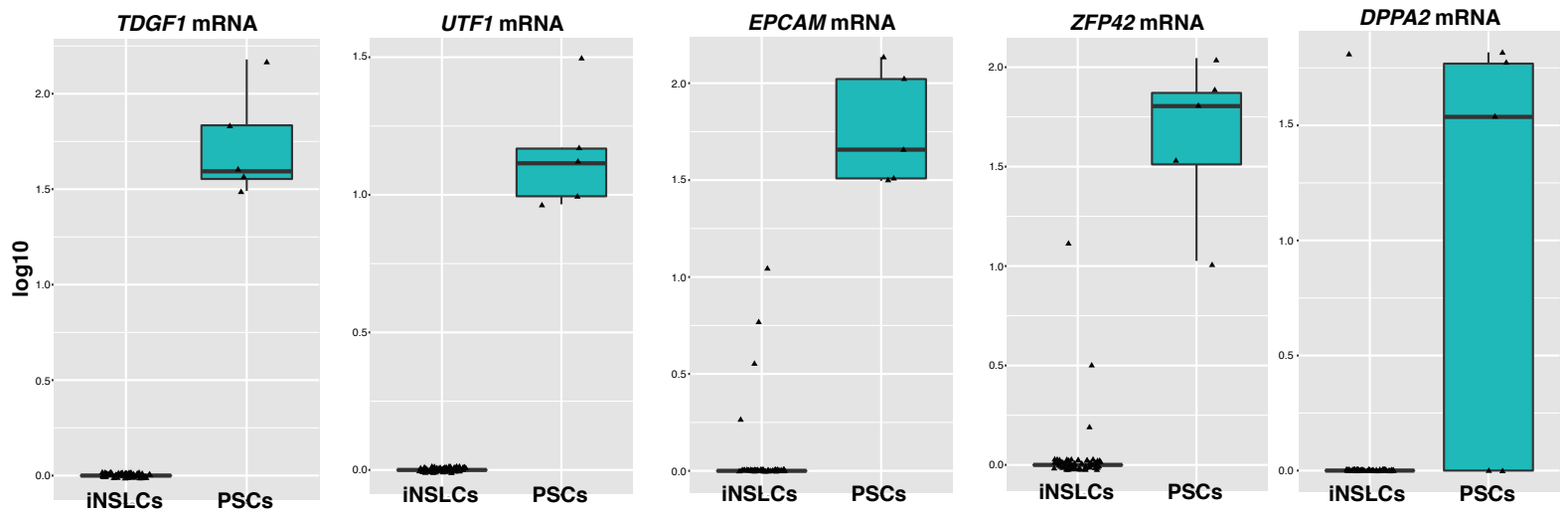
## B



## C



## D



## Supplemental Experimental Procedures

### Experimental animals.

As summarized in below, two adult marmosets (female, ages 4–6 years), four embryonic marmosets (E95–96, one male and three female), an adult beagle dog (female, 9 years old) and a post-neonatal pig (female, 1.5 months old) were used in the present study. Embryonic marmosets were obtained by Caesarian section as previously described (Shimada et al., 2012).

Animal ID (in this study)	Species	Age <sup>*1</sup>	Sex	Collected cell origin
E01F	<i>Callithrix jacchus</i> (marmoset)	E95	Female	Dorsal skin (Fibroblasts)
E02M	<i>Callithrix jacchus</i> (marmoset)	E96	Male	Dorsal skin (Fibroblasts)
I5061F	<i>Callithrix jacchus</i> (marmoset)	6.0 years old	Female	Ear skin (Fibroblasts)
CM421F	<i>Callithrix jacchus</i> (marmoset)	4.9 years old	Female	Ear skin (Fibroblasts)
CTXNS1	<i>Callithrix jacchus</i> (marmoset)	E95	Female	Cerebral cortex (Neural stem cells)
CTXNS2	<i>Callithrix jacchus</i> (marmoset)	E95	Female	Cerebral cortex (Neural stem cells)
K9	<i>Canis lupus familiaris</i> (dog)	9.0 years old	Female	Ear skin (Fibroblasts)
N01F	<i>Sus scrofa</i> (pig)	1 month old	Female	Ear skin (Fibroblasts)

\*1: Age when the fibroblasts were collected.

### Cell culture

Fibroblasts were collected from the biopsies of dorsal skin (embryonic marmoset) or ear

skin (adult marmosets, an adult dog, and a post-neonatal pig). The fibroblasts were expanded on a 0.1% gelatin-coated tissue culture dish or plate in M10 medium consisting of Dulbecco's Modified Eagle Medium supplemented with 10% inactivated fetal bovine serum and 1% Penicillin/Streptomycin solution (P/S) (all purchased from Thermo Fisher). *In vivo*-derived neural stem cells were collected from the biopsy of cerebral cortexes of embryonic marmosets and were cultured in a suspension culture using MHM medium (Shimada et al., 2012) supplemented with 2% B27, 20 ng/ml human recombinant bFGF (Thermo Fisher), 20 ng/ml human recombinant EGF (EGF; Thermo Fisher), 10 ng/ml human recombinant LIF (LIF; Nacalai Tesque) and 1 µg/ml heparin sodium salt (Nacalai Tesque).

We used three marmoset ESC lines, No. 40 and No. 20 ESCs (CMES40 and CMES20) (Sasaki et al., 2005), and DSY127 (kindly provided by Sumitomo Dainippon Pharma Co., Ltd.), which were cultured as previously described (Nii et al., 2014; Yoshimatsu et al., 2019b). In brief, the ESCs were cultured on 30 Gy-irradiated mouse embryonic fibroblasts (MEFs,  $2.5 \times 10^6$  cells / 6-well plate or 100mm dish) in ES medium (ESM). ESM consisted of 1x Knockout Dulbecco's modified Eagle's medium (Thermo Fisher) supplemented with 20% Knockout Serum Replacement (KSR; Thermo Fisher), 0.1 mM MEM Non-Essential Amino Acids Solution (NEAA; Sigma), 1 mM L-glutamine (L-glu; Thermo Fisher), 0.2 mM β-mercaptoethanol (2ME; Thermo Fisher), 1% P/S and 10 ng/ml bFGF. For passaging, the ESCs were pre-treated with 10 µM Y-27632 (Thermo Fisher) in ESM at 37°C for an hour. Then, the cells were dissociated by 0.25% trypsin-ethylenediaminetetraacetic acid (Trypsin; Nacalai Tesque), mechanically separated from MEFs, and plated onto new MEFs. Passaging was routinely performed at a 1:20 dilution in the current study.

### **Transfection, induction, and calculation of colony derivation efficiency.**

Vector transfection into fibroblasts was performed as described previously (Debowski et al., 2015; Du et al., 2015). In brief, Nucleofector 2b (Lonza) and Basic Fibroblast Nucleofector Kit (Lonza) were used for introducing a total of 3.65 µg DNA vectors into  $1 \times 10^6$  fibroblasts using V-13 condition for marmoset fibroblasts, U-23 for canine fibroblasts, T-16 for porcine fibroblasts.

For transfection into fibroblasts using the EP-A set, 0.63 µg pCE-hOCT3/4, 0.63 µg pCE-hSK, 0.63 µg pCE-hUL, 0.63 µg pCE-mp53DD, 0.63 µg pCXLE-EGFP and 0.5

$\mu\text{g}$  pCXB-EBNA1 were added to a 100  $\mu\text{l}$  nucleofection solution, which was then used for transfection using the Nucleofector 2b. For transfection into fibroblasts using the EP-B set, 0.47  $\mu\text{g}$  pCE-hOCT3/4, 0.47  $\mu\text{g}$  pCE-hSK, 0.47  $\mu\text{g}$  pCE-hUL, 0.47  $\mu\text{g}$  pCE-mp53DD, 0.47  $\mu\text{g}$  pCXLE-EGFP, 0.47  $\mu\text{g}$  pCE-K2N, 0.47  $\mu\text{g}$  pCE-KdG1 and 0.36  $\mu\text{g}$  pCXB-EBNA1 were added to a 100  $\mu\text{l}$  nucleofection solution, which was then used for transfection using the Nucleofector 2b.

The transfected fibroblasts were expanded on a 0.1% gelatin-coated tissue culture dish in M10 medium for 3–9 days following transfection. 10 ng/ml bFGF was also supplemented for transfected fibroblasts derived from adult marmosets and dog. After dissociation using Trypsin, the number of the fibroblasts and the transfection efficiency (calculated according to the EGFP fluorescence) were quantified using the Countess II FL (Thermo Fisher). Cells were then transferred onto MEFs cultured on a 0.1% gelatin-coated tissue culture 6-well plate at a density of  $1.0\text{--}10 \times 10^4$  cells per well. Twenty-four hours later, the medium was changed to 50% M10 medium and 50% NSM. After two days, the medium was changed to NSM. Medium change was performed every other day until colony picking. The induction medium NSM is composed of an 1:1 mixture of Neurobasal (Thermo Fisher) and DMEM/F-12 (Thermo Fisher), supplemented with 5% KSR, 1% N2 supplement (N2; Thermo Fisher), 2% B27 supplement (B27; Thermo Fisher), 1 mM L-glu, 1% NEAA, 0.1 mM 2-ME, 50  $\mu\text{g}/\text{ml}$  AlbuMax I (Thermo Fisher), 10 ng/ml LIF, 3  $\mu\text{M}$  CHIR99021 (CHIR; Axon Medchem), 1  $\mu\text{M}$  PD0325901 (Wako), 10  $\mu\text{M}$  Forskolin (Sigma) and 5  $\mu\text{M}$  A83-01 (Santacruz). Primary colonies were mechanically isolated or dissociated in bulk, and transferred onto new MEFs for expansion using NSM supplemented with 10  $\mu\text{M}$  Y-27632, which was removed two days after transferring. For primed conversion, early passage (P1-3) primary colony-forming cells (iNSLCs) that have been expanded were transferred onto new MEFs, and the medium was changed to ESM two days after transferring. After primed conversion for 3 weeks, iPSC colonies were mechanically picked and transferred onto new MEFs on a 24-well plate. For primed conversion of the iNSLCs derived from adult marmoset fibroblasts, 20 ng/ml Activin-A (ACTA; R&D Systems) was supplemented in the ESM during conversion. The iPSCs were cultured as described above for ESCs. Several iPSC lines were cultured in ESM supplemented with 10 ng/ml ACTA and 10 ng/ml TGF- $\beta$ 1 (Thermo Fisher) for enhancing cell growth.

Vector transfection into NSCs derived from embryonic marmosets was

performed using the NEPA21 Super Electroporator (Nepagene) as described previously for mouse NSCs (Tsuyama et al., 2015). In brief, marmoset NSCs were dissociated into single cells using TrypLE Select (Thermo Fischer). Electroporation was performed in the following condition: two poring pulses (270 V, 0.5 msec pulse length, 50 msec pulse interval and 10% decoy rate), with subsequent five transfer pulses (20V, 50 msec pulse length and interval, 40% decoy rate). We introduced a total of 11.7  $\mu\text{g}$  DNA vectors into  $1 \times 10^6$  NSCs. 1.5  $\mu\text{g}$  pCE-hOCT3/4, 1.5  $\mu\text{g}$  pCE-hSK, 1.5  $\mu\text{g}$  pCE-hUL, 1.5  $\mu\text{g}$  pCE-mp53DD, 1.5  $\mu\text{g}$  pCXLE-EGFP, 1.5  $\mu\text{g}$  pCE-K2N, 1.5  $\mu\text{g}$  pCE-KdG1 and 1.2  $\mu\text{g}$  pCXB-EBNA1 were added to 100  $\mu\text{l}$  of  $1 \times$  Opti-MEM (Thermo Fisher), which was then used for electroporation. After transfection, the cells were maintained in a suspension culture using the MHM medium supplemented with 2% B27, 20 ng/ml bFGF, 20 ng/ml EGF, 10 ng/ml LIF and 1  $\mu\text{g}/\text{ml}$  heparin sodium salt for 4 days. Then, the cells were transferred onto MEFs in the same medium. Two days later, the medium was changed to ESM.

Cell stocks of fibroblasts and iNSLCs were generated by slow-freezing using CELLBANKER1 (Zenoaq) at  $-80^\circ\text{C}$  or  $-150^\circ\text{C}$ . Cell stocks of ESCs and iPSCs were generated by vitrification using Cell Reservoir One for vitrification (Nacalai Tesque) in liquid  $\text{N}_2$ .

The derivation efficiency (%) was calculated as follows: (number of colonies / number of EGFP-positive transfected fibroblasts passaged onto MEFs)  $\times$  100.

## **Nomenclature**

Marmoset ID (Table S1) and vector set (Fig. 1A) were used to name marmoset iNSLC (cjiNSLC) lines. For example, "cjiNSLC E01F A-2" corresponds to a marmoset iNSLC line which was derived from the fibroblasts of the E01F marmoset by using the EP-A vector set, while "cjiNSLC E02M B-0" corresponds to bulk iNSLCs derived from the fibroblasts of the E02M marmoset by using the EP-B vector set (without mechanical isolation of a colony).

Marmoset ID, vector set, and clone number of the parental iNSLC line were used to name marmoset iPSC (cjiPSC) lines. For example, "cjiPSC E01F A-2-2" corresponds to a marmoset iPSC line which was converted from the cjiNSLC E01F A-2. However, for the iPSC lines converted from bulk iNSLCs, "0" was used as the clone number of the parental iNSLC line. For example, "cjiPSC E02M B-0-7" was converted from bulk iNSLCs which were derived from E02M fibroblasts using the EP-B vector set.

## Vector construction

Vectors used for reprogramming are summarized in Figure 1A. In the EP-B set, two novel episomal vectors, pCE-K2N and pCE-KdG1, were constructed using the expression-cassette-excised pCE-hUL as a backbone (pCE backbone). For constructing pCE-K2N, the *KLF2-F2A-NANOG* fragment was amplified by PCR from the pPB-C6F/TdTomato vector (Addgene #140826) (Kisa et al., 2017), and inserted into the pCE backbone. For constructing pCE-KdG1, the entire coding sequence of the marmoset *KDM4D* (single exon gene) was amplified from the genomic DNA, and fused to the human *GLIS1*, which was amplified from pCXLE-GLIS1 (kindly provided by Shinya Yamanaka) via a *Thoseaasigna* virus self-cleaving 2A peptide sequence (T2A), and inserted into the pCE backbone.

Vectors used for PGCLC experiments are shown in Figure S5A and S5D. Construction of the *BLIMP1-Venus* and *VASA-tdTomato* vectors (Figure S5A) were described previously (Yoshimatsu et al., 2019c). For construction of pPBCAG-rtTAM2-2A-SOX17GR-IH (Figure S5D, top), *T2A-SOX17-GR* was inserted into SmaI/NotI-digested pPBCAG-rtTAM2-IH (Addgene #140827) (Kisa et al., 2017) by Seamless cloning using GeneArt™ Seamless PLUS Cloning and Assembly Kit (Thermo Fisher). The *T2A-SOX17-GR* fragment was composed of *T2A* (a self-cleaving 2A peptide sequence from *Thosea asigna* virus capsid protein), human *SOX17* fused to the I747T-mutant ligand binding domain (500 – 777 aa) of the human *glucocorticoid receptor (GR)* gene (Brocard et al., 1998). pPB-tet-PH-PRDM1 (Figure S5D, bottom) contained the human *PRDM1 (BLIMP1)* gene under the control of tetracycline-responsive promoter element with a Puromycin resistance cassette, which was kindly provided by Drs. Yuhki Nakatake and Minoru Ko (Keio University).

pCE-K2N, pCE-KdG1 and pPBCAG-rtTAM2-2A-SOX17GR-IH have been deposited into Addgene (<https://www.addgene.org>; #154879, #154880 and #165079).

## qPCR and RT-PCR

Extraction of total cellular RNA, reverse transcription and quantitative reverse transcription PCR (qPCR) analysis were performed as previously described (Kisa et al., 2017). For quantification of gene expression, we utilized a relative standard curve method. *GAPDH* was used as the internal control. All qPCR data was biologically and technically



triplicated. Expression level of each gene in No. 40 cjESCs was set to 1.0 in the qPCR analysis. Reverse transcription PCR (RT-PCR) analysis was performed using the TaKaRa Ex Taq (Takara) according to the manufacturer's introductions. In brief, 1× ExTaq Buffer, 0.4 mM each dNTP, 5 μM each primer, 0.5% ExTaq and 5% cDNA (reverse-transcribed from 4 ng/μl RNA) were diluted in nuclease-free water, and PCR was performed under the following condition: 95°C 20 sec, 30 repeats of 95°C 30 sec and 60°C 1 min, and then kept at 4°C until gel electrophoresis. Primers are listed in the next page.

### Genomic PCR

For genomic PCR, cells were lysed overnight at 55°C in Cell Lysis Buffer consisting of 0.2 M Tris-HCl, 10 mM EDTA, 0.2% SDS and 0.2 M NaCl in nuclease-free water with 10 μg/ml Proteinase K. Genomic DNA was purified by a standard method using phenol-chloroform and ethanol, and subsequently diluted in TE buffer. PrimeSTAR Max DNA Polymerase (Takara) was used for genotyping PCR according to the manufacturer's introductions. In brief, a total 10 μl PCR solution consisted of 100 ng genomic DNA, 5 μl 2x PrimeSTAR Max DNA Polymerase, 1.6 μM each primer, 2% DMSO in nuclease-free water. PCR was performed under the following condition: 94°C 30 sec, 45 repeats of 98°C 10 sec and 68°C 1 min, followed by 68°C 10 min and then kept at 4°C until electrophoresis using 1% agarose gel. For the detection of residual episomal vectors, 0.5 ng of each episomal vector (pCE-hUL for the detection of OriP) was used as a positive control. Primers are listed below.

Gene*, reference	Usage	Sequence	Amplicon size
cj+hs+clf+ss <i>GAPDH</i> (Yoshimatsu et al., 2019b)	qPCR, RT-PCR	GCACCGTCAAGGCTGAGAAC	138 bp
		TGGTGAAGACGCCAGTGGA	
cj <i>OCT4</i>	qPCR	GCAAGCCCTCATTTCACCAG	77 bp
		CAAAATCCGAAGCCAGGTGTC	
	qPCR	GGAGGAAGCTGACAACAATGAAA	64 bp

cj+hs <i>OCT4</i> (Yoshimatsu et al., 2019b)		GGCCTGCACGAGGGTTT	
cj <i>NANOG</i> (Yoshimatsu et al., 2019b)	qPCR	ACGAACATGCCACCTGAAGA TACGAGGAAGGGGAGGAGGT	107 bp
cj+hs <i>NANOG</i>	qPCR	GCCTGGAGCAGTCCCTTCTA TCCAAGTCACTGGCAGGAGA	89 bp
cj <i>SOX2</i>	qPCR	ACAGTTGCAAACGTGGAGAGAAG ACCACAGAGATGGTTTGCCAGTA	109 bp
cj <i>KLF4</i>	qPCR	CCCAGCTGAGTCAACTTGTGAG ACCCCTTGGCATTGTAAGT	155 bp
cj+hs <i>KLF4</i>	qPCR	AAGAGTTCCCATCTCAAGGCACA GGGCGAATTTCCATCCACAG	91 bp
cj <i>ZFP42</i>	qPCR	CAAGCTCCCTTCTGGAATGTTCT TTCTGCGAGCTGTTTAGGATCTG	176 bp
cj <i>DPPA5</i>	qPCR	ATCCAGAAGTGTTCCAGGTCCAG CAGTTCATCCAAGGGCTCAGTT	286 bp
cj+hs <i>TERT</i>	qPCR	AGAGTGTCTGGAGCAAGTTGC CGTAGTCCATGTTTACAATCG	183 bp
cj <i>LIN28</i>	qPCR	GCACAGGGAAAGCCAACA GTGATGGTGTGAACCCCAAC	216 bp
cj+hs <i>LIN28</i> (Piskounova et al., 2011)	qPCR	AAGCGCAGATCAAAAGGAGA CTGATGCTCTGGCAGAAGTG CTTCGTGCCTACCCTTTTCAAGT	113 bp
clf <i>OCT4</i>	RT-PCR	CCCTCTGTGTCTGTCACCACTCT TCTACACCCTTTGTGTTCCAGA	184 bp
clf <i>NANOG</i>	RT-PCR	TTCCAGCAAAATTCTATGGGTGA TAATGGGACACTATCGAGGCAGA	253 bp
clf <i>SOX2</i>	RT-PCR	ACAGTTGCAAACGTGGAAAAGAA AACCTGTATGGCCATTTTGTCTT	197 bp
ss <i>OCT4</i>	RT-PCR	CGGAAGAGAAAGCGGACAAGTAT	199 bp

		CTCGTTGCGAATAGTCACTGCTT	
ss <i>NANOG</i>	RT-PCR	TCTTCACCAATGCCTGAGGTTTA TGAATAAGCAGATCCATGGAGGA	125 bp
ss <i>SOX2</i>	RT-PCR	CCACCTACAGCATGTCCTACTCG CCTGGAGTGGGAAGAAGAGGTAA AACTTTCTGCAAAGCTCCTACCG	125 bp
cj+hs+clf <i>GAPDH</i> locus	Genomic PCR	GCACCGTCAAGGCTGAGAAC TGGTGAAGACGCCAGTGGA	138 bp
cj+hs+clf <i>OCT4</i> locus	Genomic PCR	GGAGGAAGCTGACAACAATGAAA GGCCTGCACGAGGGTTT	341 bp
ss <i>OCT4</i> locus	Genomic PCR	CGGAAGAGAAAGCGGACAAGTAT CTCGTTGCGAATAGTCACTGCTT	298 bp
OriP (Yu et al., 2009)	Genomic PCR	TTCCACGAGGGTAGTGAACC TCGGGGGTGTTAGAGACAAC	544 bp
cj+hs <i>SRY</i> locus	Genomic PCR	AACGTCCAGGATAGAGTGAAGCGA CTTCCGACGAGGTCGATACTTATA	240 bp
OC: CAG-OCT4 (pCE-hOCT3/4)	Genomic PCR	TGCTAACCATGTTTCATGCCTTCT AAATTCTCCAGGTTGCCTCTCAC	844 bp
SK: SOX2-KLF4 (pCE-hSK)	Genomic PCR	ACTTCACATGTCCCAGCACTACC ATCGTTGAACTCCTCGGTCTCTC	469 bp
UL: LMYC-Lin28 (pCE-hUL)	Genomic PCR	CAGCAGCAGTTGCAGAAAAGAAT TAAAGGTGAACTCCACTGCCTCA	448 bp
MP: mp53DD (pCE-mp53DD)	Genomic PCR	CACAGTCGGATATCAGCCTCAAG TAGACTGGCCCTTCTTGGTCTTC	237 bp
KN: CAG-KLF2 (pCE-K2N)	Genomic PCR	TGCTAACCATGTTTCATGCCTTCT AGGGCTTCTCACCTGTGTGC	1001 bp
KG: KDM4D-GLIS1 (pCE-KdGI)	Genomic PCR	GAAGTCGAGTTGCCTAGGAGAGC CGGAGTCCATTTACACAGGTGAC	851 bp

\*Primers specific for each species are indicated as cj, *Callithrix jacchus* (marmoset); hs, *Homo sapiens* (human); clf, *Canis lupus familiaris* (dog); ss, *Sus scrofa* (pig). All primers are designed not to amplify murine cDNA/genomic DNA sequences.

### **Three-germ-layer differentiation assay**

For *in vivo* three-germ-layer differentiation assay, teratoma formation was performed as previously described (Tomioka et al., 2010). Teratomas were fixed with 4% PFA and subjected to Hematoxylin-Eosin staining or Hematoxylin staining with immunocytochemical staining using an anti-Neurofilament 200kDa antibody (MAB5262; Merck).

For *in vitro* three-germ-layer differentiation assay, iPSCs were detached from MEFs *en bloc*, and transferred to a suspension culture for two weeks using M10 medium or EB medium (Yoshimatsu et al., 2019b). For further differentiation, the cells were plated onto poly-L-ornithine/fibronectin-coated glass coverslips for an additional two weeks in the same medium.

Direct neurosphere formation assay was performed as following: ESCs, iPSCs and iNSLCs were detached from MEFs and transferred to a suspension culture in MHM medium (Shimada et al., 2012) supplemented with 2% B27. After one week of suspension culture at which point primary neurospheres were formed, the cells were plated onto poly-L-ornithine/fibronectin-coated glass coverslips for an additional week of culture in the same medium.

For deriving gliogenic cells by the direct neurosphere formation assay, primary neurospheres were dissociated into single cells using TrypLE Select and transferred to a suspension culture in the same medium for an additional week to enable secondary neurosphere formation. Then, the cells were plated onto poly-L-ornithine/fibronectin-coated glass coverslips for one week of culture in the same medium. For posteriorization/ventralization of the iNSLCs, 1  $\mu$ M retinoic acid (Tocris Bioscience), 2  $\mu$ M Purmorphamine (Merck) and 3  $\mu$ M CHIR were supplemented in the medium during secondary neurosphere formation, followed by an adherent culture in the same medium for one week.

### **Generation of PGC-reporter iPSCs, PGCLC induction and FACS**

The generation of marmoset iPSCs (E01F A-2-2) harboring *BLIMP1-Venus* and *VASA-tdTomato* reporters was performed as described previously (Yoshimatsu et al., 2020; Yoshimatsu et al., 2019c). In brief, the iPSCs were transfected with 8  $\mu$ g of pUC-DEST-cjBLIMP1-Venus-HygTK (Addgene #141028) and 2  $\mu$ g of PX459 (Addgene #48139) containing single-guide RNA sequence for the marmoset PRDM1 gene

(GGAAAATCTTAAGGATCCAT) by lipofection, and subsequently selected in the presence of Hygromycin (25 µg/ml) for two weeks. Then, Hygromycin-resistant iPSC colonies were mechanically isolated and clonally expanded for genotyping PCR (Figure S5B, top). Next, the #8 (BV8) iPSC clone was transfected with 2 µg of pCMV-HyPBase (kindly provided by Dr. Kosuke Yusa, Sanger Institute) and 2 µg of pPB-VASA-tdTomato-pNeo, and subsequently selected in the presence of G418 (50 µg/ml) and Ganciclovir (1 µM). Then, resistant iPSC colonies were mechanically isolated and clonally expanded for PCR (Figure S5B, bottom). The #1 (BV8VT1) iPSC clone was used for further experiments.

For generation of marmoset ESCs and iPSCs with dexamethasone/doxycycline-inducible *SOX17/BLIMP1* transgenes, cells were transfected with 4 µg of pPBCAG-rtTAM2-2A-SOX17GR-IH, 4 µg of pPB-tet-PH-PRDM1 (Figure S5D) and 2 µg of pCMV-HyPBase (kindly provided by Dr. Kosuke Yusa) by lipofection as described previously (Yoshimatsu et al., 2019c), and subsequently selected in the presence of Puromycin (1 µg/ml) and Hygromycin (25 µg/ml) for two weeks.

The timetable of PGCLC induction is shown in Figure S5C. In brief, sub-confluent marmoset ESCs and iPSCs were dissociated using Trypsin, then plated onto a Poly-L-Ornithine (Sigma)-coated well without any dilution in Medium 1 (Day 0). The Medium 1 consisted of GK15 or  $\alpha$ RB27 (GK15 for No. 40 ESCs and E01F A-2-2 iPSCs,  $\alpha$ RB27 for DSY127 ESCs) (Sakai et al., 2020) supplemented with 100 ng/ml ACTA, 2 µg/ml Dexamethasone (Dex) and 10 µM Y-27632. The cells were cultured in the same medium until Day 4. Medium change was performed every other day. Supplementation of 3 µM CHIR was performed on Day 3.5. On Day 4, the cells were detached into single cells using TrypLE Select, then suspended in Medium 2, and  $1 \times 10^4$  cells were aggregated in low attachment V-shaped 96-well plates (100 µl/well, Sumitomo Bakelite). The Medium 2 consisted of GK15 or  $\alpha$ RB27 (GK15 for No. 40 ESCs and E01F A-2-2 iPSCs,  $\alpha$ RB27 for DSY127 ESCs) supplemented with 500 ng/ml human recombinant BMP4, 100 ng/ml SCF, 50 ng/ml EGF, 10 ng/ml LIF, 2 µg/ml Dex, 2 µg/ml Doxycycline (Dox) and 10 µM Y-27632. Following single-cell dissociation of Day10-differentiated cells using Accutase (Nacalai Tesque), BLIMP1-Venus positive cells (detected by the FITC filter) were sorted using a Cell Sorter SH800Z (Sony Biotechnology). 7-AAD (Thermo Fisher) was used for the removal of dead cells (detected by APC filter).

### **Alkaline phosphatase staining and immunocytochemistry.**

For alkaline phosphatase (AP) staining, cells were fixed with 100% ethanol for 10 min at room temperature (RT). AP staining was performed using the SIGMAFAST™ BCIP®/NBT (Sigma) according to the manufacturer's introductions.

For immunocytochemical analysis, cells were fixed with 4% paraformaldehyde (PFA) for 15-30 min at room temperature. After incubating with blocking buffer (PBS containing 0.05% Tween 20 (Sigma) and 10% goat or donkey serum) for 30–60 min at RT, the cells were incubated with primary antibodies at 4°C overnight. After incubation with primary antibodies, the cells were washed with PBS three times, and incubated with Alexa488-, Alexa555-, or Alexa647-conjugated secondary antibodies (Thermo Fisher) and 10 mg/ml Hoechst 33258 (Sigma) for one hour at RT. Primary antibodies used in this study were as follows: OCT4 (1:200; H134; Santa Cruz), NANOG (1:500; 1E6C4; Cell Signaling), SOX2 (1:200; AF1979; R&D Systems), SSEA3 (1:500, ab16286, Abcam), SSEA4 (1:500; MAB4304; Merck, TRA-1-60 (1:500; MAB4360; Merck), TRA-1-81 (1:500, MAB4381, Merck),  $\beta$ III-tubulin (1:400; 2G10; Abcam), MAP2 (1:500; AB5392; Abcam), PAX6 (1:500; PD022, MBL), MSII (1:500; D270-3; MBL),  $\alpha$ SMA (1:1000; 1A4; Sigma), SOX17 (1:200; AF1924; R&D Systems), HNF3 $\beta$ /FOXA2 (1:500; D5606; Cell Signaling) , ChAT (1:300, Aves Labs), Islet1 (1:300, 39.4D5, DSHB), Galactocerebroside (1:1000, MAB342, Merck), GFAP (1:300, BT-575, Biomedical Technologies), Doublecortin (1:200, AB5910, Merck).

**Karyotyping.** Q-banding and G-banding-based karyotyping analyses were performed by Chromosome Science Labo. Ltd. (<http://www.chromoscience.jp>)

### **3'IVT microarray analysis.**

Extraction of total cellular RNA was performed as described above. Microarray analysis was performed using the GeneChip Marmoset Gene 1.0 ST Array (Thermo Fisher), which is specific for mRNAs (3'IVT; designed for exons in 3' side) of marmoset genes (33,971 genes were analyzed using 656,668 probes in total), according to the manufacturer's introductions. The microarray data was analyzed using the GeneSpring software (Agilent).

### **Bulk mRNA-seq analysis.**

Poly(A)+ RNA was selected and converted to a library of cDNA fragments (mean length: 350 bp) with adaptors attached to both ends for sequencing using the KAPA mRNA Capture Kit (KK8440; Kapa Biosystems), KAPA RNA HyperPrep Kit (KK8542; Kapa Biosystems), KAPA Pure Beads (KK8543; Kapa Biosystems) and SeqCap Adapter Kit A (Roche) according to the manufacturer's instructions. The cDNA libraries were quantified using the KAPA Library Quantification Kits (KK4828; Kapa Biosystems), and were sequenced using an Illumina HiSeqX to obtain 150-nucleotide sequences (paired-end). Data of mRNA-seq (*fastq* file format) were quality-checked, and low-quality reads (score < 30), adapter sequences, and overrepresented sequences such as poly-A chain were trimmed using the *Trim Galore!* (ver.0.4.0). The remaining reads were mapped to the *Homo sapiens* (hg19), *Callithrix jacchus* (cj3.2.1.86), *Canis lupus familiaris* (CanFam3.1) and *Sus scrofa* (Sscrofa11.1) genome using the *STAR* (ver.2.5.3a) (Dobin and Gingeras, 2015), and the output file (BAM file format) were summarized using the *featureCounts* (1.5.2) (Liao et al., 2014). The summarized data were processed by the *DESeq2* (3.3.0) (Love et al., 2014) for estimating their size factors, followed by the removal of reads not expressed in any of the samples. Subsequently, the data were normalized by varianceStabilizingTransformation (vst).

For mRNA-seq analysis, we also included deposited data of previous studies in GEO (<https://www.ncbi.nlm.nih.gov/geo/>) and DDBJ (<https://www.ddbj.nig.ac.jp/>) as following: marmoset ESCs (No40\_ES\_P63, DSY127\_ES\_P17, No20\_ES\_P45) and iPSCs (RNAiPS\_1) in GSE152259 (Nakajima et al., 2019); marmoset ESCs (cjes001\_P83, P91, P94) and iPSCs (DPZcj\_iPSC1\_P18, P19, P22, P24) in GSE64966 (Debowski et al., 2015); adult marmoset cortex in GSE152264 (Yoshimatsu et al., 2019a), marmoset early-stage embryos in GSE138944 (Shiozawa et al., 2020); porcine iPSCs and early-stage embryos: GSE92889 (Secher et al., 2017); human ESCs in ERA260913 (Chan et al., 2013).

We have deposited mRNA-seq data of the present study in The Gene Expression Omnibus database of NIH (<https://www.ncbi.nlm.nih.gov/geo/>), and the accession number is GSE152493.

### **Single-cell RamDA-seq analysis.**

Single-cell RamDA cDNA library was prepared using GenNext® RamDA-seq™ Single Cell Kit (Toyobo) and Nextera XT DNA Library Preparation Kit (Illumina)

according to the manufacturer's introductions. Single cell sorting was performed using a Cell Sorter SH800Z (Sony Biotechnology). For sorting, FITC Mouse anti-Human TRA-1-60 Antigen (BD) for marmoset ESCs and iPSCs, and Alexa Fluor 647 Mouse anti-Human Alkaline Phosphatase (BD) for marmoset iNSLCs were used for the removal of MEF contamination. In addition, 7-AAD (Thermo Fisher) was used for the removal of dead cells. Libraries were sequenced using an Illumina HiSeq 2000 to obtain 150-nucleotide sequences (paired-end). Sequenced reads were trimmed using *trimmomatic* based on the quality of reads and adaptor sequences. The remaining reads were mapped to the *Callithrix jacchus* (cj1700) genome using *STAR*, and gene expression level were counted using the (1.5.2). Normalization and downstream analysis were conducted using the *R* software.

### Statistical analysis

All data were expressed as means  $\pm$  S.E.M. The statistical significance of differences was analyzed by Student's *t*-test. Differences of  $p < 0.05$  were showed as \*,  $p < 0.01$  were showed as \*\* and  $p < 0.001$  were showed as \*\*\*, which were considered statistically significant.

### Supplementary References

Brocard, J., Feil, R., Chambon, P., and Metzger, D. (1998). A chimeric Cre recombinase inducible by synthetic, but not by natural ligands of the glucocorticoid receptor. *Nucleic Acids Res* 26, 4086-4090.

Campolo, F., Gori, M., Favaro, R., Nicolis, S., Pellegrini, M., Botti, F., Rossi, P., Jannini, E.A., and Dolci, S. (2013). Essential role of Sox2 for the establishment and maintenance of the germ cell line. *Stem Cells* 31, 1408-1421.

Chan, Y.S., Goke, J., Ng, J.H., Lu, X., Gonzales, K.A., Tan, C.P., Tng, W.Q., Hong, Z.Z., Lim, Y.S., and Ng, H.H. (2013). Induction of a human pluripotent state with distinct regulatory circuitry that resembles preimplantation epiblast. *Cell Stem Cell* 13, 663-675.

Chow, L., Johnson, V., Regan, D., Wheat, W., Webb, S., Koch, P., and Dow, S. (2017). Safety and immune regulatory properties of canine induced pluripotent stem cell-derived mesenchymal stem cells. *Stem Cell Res* 25, 221-232.

Cong, X., Zhang, S.M., Ellis, M.W., and Luo, J. (2019). Large Animal Models for the Clinical Application of Human Induced Pluripotent Stem Cells. *Stem Cells Dev* 28, 1288-



1298.

Debowski, K., Warthemann, R., Lentjes, J., Salinas-Riester, G., Dressel, R., Langenstroth, D., Gromoll, J., Sasaki, E., and Behr, R. (2015). Non-viral generation of marmoset monkey iPS cells by a six-factor-in-one-vector approach. *PLoS One* *10*, e0118424.

Di Stefano, B., Prigione, A., and Broccoli, V. (2009). Efficient genetic reprogramming of unmodified somatic neural progenitors uncovers the essential requirement of Oct4 and Klf4. *Stem Cells Dev* *18*, 707-716.

Dobin, A., and Gingeras, T.R. (2015). Mapping RNA-seq Reads with STAR. *Current protocols in bioinformatics* *51*, 11.14.11-19.

Du, X., Feng, T., Yu, D., Wu, Y., Zou, H., Ma, S., Feng, C., Huang, Y., Ouyang, H., Hu, X., *et al.* (2015). Barriers for Deriving Transgene-Free Pig iPS Cells with Episomal Vectors. *Stem Cells* *33*, 3228-3238.

Esteban, M.A., Xu, J., Yang, J., Peng, M., Qin, D., Li, W., Jiang, Z., Chen, J., Deng, K., Zhong, M., *et al.* (2009). Generation of induced pluripotent stem cell lines from Tibetan miniature pig. *J Biol Chem* *284*, 17634-17640.

Ezashi, T., Telugu, B.P., Alexenko, A.P., Sachdev, S., Sinha, S., and Roberts, R.M. (2009). Derivation of induced pluripotent stem cells from pig somatic cells. *Proc Natl Acad Sci U S A* *106*, 10993-10998.

Gao, X., Nowak-Imialek, M., Chen, X., Chen, D., Herrmann, D., Ruan, D., Chen, A.C.H., Eckersley-Maslin, M.A., Ahmad, S., Lee, Y.L., *et al.* (2019). Establishment of porcine and human expanded potential stem cells. *Nat Cell Biol* *21*, 687-699.

Hatoya, S., Torii, R., Kondo, Y., Okuno, T., Kobayashi, K., Wijewardana, V., Kawate, N., Tamada, H., Sawada, T., Kumagai, D., *et al.* (2006). Isolation and characterization of embryonic stem-like cells from canine blastocysts. *Mol Reprod Dev* *73*, 298-305.

Hou, P., Li, Y., Zhang, X., Liu, C., Guan, J., Li, H., Zhao, T., Ye, J., Yang, W., Liu, K., *et al.* (2013). Pluripotent stem cells induced from mouse somatic cells by small-molecule compounds. *Science* *341*, 651-654.

Irie, N., Weinberger, L., Tang, W.W., Kobayashi, T., Viukov, S., Manor, Y.S., Dietmann, S., Hanna, J.H., and Surani, M.A. (2015). SOX17 is a critical specifier of human primordial germ cell fate. *Cell* *160*, 253-268.

Kim, J., Efe, J.A., Zhu, S., Talantova, M., Yuan, X., Wang, S., Lipton, S.A., Zhang, K., and Ding, S. (2011). Direct reprogramming of mouse fibroblasts to neural progenitors. *Proc Natl Acad Sci U S A* *108*, 7838-7843.

Kim, J.B., Greber, B., Arauzo-Bravo, M.J., Meyer, J., Park, K.I., Zaehres, H., and Scholer, H.R. (2009a). Direct reprogramming of human neural stem cells by OCT4. *Nature* *461*, 649-643.

Kim, J.B., Sebastiano, V., Wu, G., Arauzo-Bravo, M.J., Sasse, P., Gentile, L., Ko, K., Ruau, D., Ehrich, M., van den Boom, D., *et al.* (2009b). Oct4-induced pluripotency in adult neural stem cells. *Cell* *136*, 411-419.

Kim, J.B., Zaehres, H., Wu, G., Gentile, L., Ko, K., Sebastiano, V., Arauzo-Bravo, M.J., Ruau, D., Han, D.W., Zenke, M., *et al.* (2008). Pluripotent stem cells induced from adult neural stem cells by reprogramming with two factors. *Nature* *454*, 646-650.

Kisa, F., Shiozawa, S., Oda, K., Yoshimatsu, S., Nakamura, M., Koya, I., Kawai, K., Suzuki, S., and Okano, H. (2017). Naive-like ESRRB(+) iPSCs with the Capacity for Rapid Neural Differentiation. *Stem Cell Reports* *9*, 1825-1838.

Kobayashi, T., Zhang, H., Tang, W.W.C., Irie, N., Withey, S., Klisch, D., Sybirna, A., Dietmann, S., Contreras, D.A., Webb, R., *et al.* (2017). Principles of early human development and germ cell program from conserved model systems. *Nature* *546*, 416-420.

Lee, A.S., Xu, D., Plews, J.R., Nguyen, P.K., Nag, D., Lyons, J.K., Han, L., Hu, S., Lan, F., Liu, J., *et al.* (2011). Preclinical derivation and imaging of autologously transplanted canine induced pluripotent stem cells. *J Biol Chem* *286*, 32697-32704.

Liao, Y., Smyth, G.K., and Shi, W. (2014). featureCounts: an efficient general purpose program for assigning sequence reads to genomic features. *Bioinformatics (Oxford, England)* *30*, 923-930.

Love, M.I., Huber, W., and Anders, S. (2014). Moderated estimation of fold change and dispersion for RNA-seq data with DESeq2. *Genome biology* *15*, 550.

Lu, J., Liu, H., Huang, C.T., Chen, H., Du, Z., Liu, Y., Sherafat, M.A., and Zhang, S.C. (2013). Generation of integration-free and region-specific neural progenitors from primate fibroblasts. *Cell Rep* *3*, 1580-1591.

Luo, J., Suhr, S.T., Chang, E.A., Wang, K., Ross, P.J., Nelson, L.L., Venta, P.J., Knott, J.G., and Cibelli, J.B. (2011). Generation of leukemia inhibitory factor and basic fibroblast growth factor-dependent induced pluripotent stem cells from canine adult somatic cells. *Stem Cells Dev* *20*, 1669-1678.

Nakajima, M., Yoshimatsu, S., Sato, T., Nakamura, M., Okahara, J., Sasaki, E., Shiozawa, S., and Okano, H. (2019). Establishment of induced pluripotent stem cells from common

marmoset fibroblasts by RNA-based reprogramming. *Biochem Biophys Res Commun* 515, 593-599.

Nakajima-Koyama, M., Lee, J., Ohta, S., Yamamoto, T., and Nishida, E. (2015). Induction of Pluripotency in Astrocytes through a Neural Stem Cell-like State. *J Biol Chem* 290, 31173-31188.

Nii, T., Marumoto, T., Kawano, H., Yamaguchi, S., Liao, J., Okada, M., Sasaki, E., Miura, Y., and Tani, K. (2014). Analysis of essential pathways for self-renewal in common marmoset embryonic stem cells. *FEBS Open Bio* 4, 213-219.

Nishimura, T., Hatoya, S., Kanegi, R., Wijesekera, D.P.H., Sanno, K., Tanaka, E., Sugiura, K., Hiromitsu Tamada, N.K., Imai, H., and Inaba, T. (2017). Feeder-independent canine induced pluripotent stem cells maintained under serum-free conditions. *Mol Reprod Dev* 84, 329-339.

Ogorevc, J., Orehek, S., and Dovc, P. (2016). Cellular reprogramming in farm animals: an overview of iPSC generation in the mammalian farm animal species. *J Anim Sci Biotechnol* 7, 10.

Ohinata, Y., Ohta, H., Shigeta, M., Yamanaka, K., Wakayama, T., and Saitou, M. (2009). A signaling principle for the specification of the germ cell lineage in mice. *Cell* 137, 571-584.

Piskounova, E., Polyarchou, C., Thornton, J.E., LaPierre, R.J., Pothoulakis, C., Hagan, J.P., Iliopoulos, D., and Gregory, R.I. (2011). Lin28A and Lin28B inhibit let-7 microRNA biogenesis by distinct mechanisms. *Cell* 147, 1066-1079.

Sakai, Y., Nakamura, T., Okamoto, I., Gyobu-Motani, S., Ohta, H., Yabuta, Y., Tsukiyama, T., Iwatani, C., Tsuchiya, H., Ema, M., *et al.* (2020). Induction of the germ cell fate from pluripotent stem cells in cynomolgus monkeys. *Biol Reprod* 102, 620-638.

Sasaki, E., Hanazawa, K., Kurita, R., Akatsuka, A., Yoshizaki, T., Ishii, H., Tanioka, Y., Ohnishi, Y., Suemizu, H., Sugawara, A., *et al.* (2005). Establishment of novel embryonic stem cell lines derived from the common marmoset (*Callithrix jacchus*). *Stem Cells* 23, 1304-1313.

Sasaki, K., Nakamura, T., Okamoto, I., Yabuta, Y., Iwatani, C., Tsuchiya, H., Seita, Y., Nakamura, S., Shiraki, N., Takakuwa, T., *et al.* (2016). The Germ Cell Fate of Cynomolgus Monkeys Is Specified in the Nascent Amnion. *Dev Cell* 39, 169-185.

Sasaki, K., Yokobayashi, S., Nakamura, T., Okamoto, I., Yabuta, Y., Kurimoto, K., Ohta, H., Moritoki, Y., Iwatani, C., Tsuchiya, H., *et al.* (2015). Robust In Vitro Induction of

Human Germ Cell Fate from Pluripotent Stem Cells. *Cell Stem Cell* 17, 178-194.

Schneider, M.R., Adler, H., Braun, J., Kienzle, B., Wolf, E., and Kolb, H.J. (2007). Canine embryo-derived stem cells--toward clinically relevant animal models for evaluating efficacy and safety of cell therapies. *Stem Cells* 25, 1850-1851.

Secher, J.O., Ceylan, A., Mazzoni, G., Mashayekhi, K., Li, T., Muenthaisong, S., Nielsen, T.T., Li, D., Li, S., Petkov, S., *et al.* (2017). Systematic in vitro and in vivo characterization of Leukemia-inhibiting factor- and Fibroblast growth factor-derived porcine induced pluripotent stem cells. *Mol Reprod Dev* 84, 229-245.

Shimada, H., Nakada, A., Hashimoto, Y., Shigeno, K., Shionoya, Y., and Nakamura, T. (2010). Generation of canine induced pluripotent stem cells by retroviral transduction and chemical inhibitors. *Mol Reprod Dev* 77, 2.

Shimada, H., Okada, Y., Ibata, K., Ebise, H., Ota, S., Tomioka, I., Nomura, T., Maeda, T., Kohda, K., Yuzaki, M., *et al.* (2012). Efficient derivation of multipotent neural stem/progenitor cells from non-human primate embryonic stem cells. *PLoS One* 7, e49469.

Shiozawa, S., Nakajima, M., Okahara, J., Kuortaki, Y., Kisa, F., Yoshimatsu, S., Nakamura, M., Koya, I., Yoshimura, M., Sasagawa, Y., *et al.* (2020). Primed to naive-like conversion of the common marmoset embryonic stem cells. *Stem Cells Dev*.

Takahashi, K., Tanabe, K., Ohnuki, M., Narita, M., Sasaki, A., Yamamoto, M., Nakamura, M., Sutou, K., Osafune, K., and Yamanaka, S. (2014). Induction of pluripotency in human somatic cells via a transient state resembling primitive streak-like mesendoderm. *Nat Commun* 5, 3678.

Tomioka, I., Maeda, T., Shimada, H., Kawai, K., Okada, Y., Igarashi, H., Oiwa, R., Iwasaki, T., Aoki, M., Kimura, T., *et al.* (2010). Generating induced pluripotent stem cells from common marmoset (*Callithrix jacchus*) fetal liver cells using defined factors, including Lin28. *Genes Cells* 15, 959-969.

Tsukamoto, M., Nishimura, T., Yodoe, K., Kanegi, R., Tsujimoto, Y., Alam, M.E., Kuramochi, M., Kuwamura, M., Ohtaka, M., Nishimura, K., *et al.* (2018). Generation of Footprint-Free Canine Induced Pluripotent Stem Cells Using Auto-Erasable Sendai Virus Vector. *Stem Cells Dev* 27, 1577-1586.

Tsuyama, J., Bunt, J., Richards, L.J., Iwanari, H., Mochizuki, Y., Hamakubo, T., Shimazaki, T., and Okano, H. (2015). MicroRNA-153 Regulates the Acquisition of Gliogenic Competence by Neural Stem Cells. *Stem Cell Reports* 5, 365-377.

Wang, L., Wang, L., Huang, W., Su, H., Xue, Y., Su, Z., Liao, B., Wang, H., Bao, X., Qin, D., *et al.* (2013). Generation of integration-free neural progenitor cells from cells in human urine. *Nat Methods* *10*, 84-89.

West, F.D., Uhl, E.W., Liu, Y., Stowe, H., Lu, Y., Yu, P., Gallegos-Cardenas, A., Pratt, S.L., and Stice, S.L. (2011). Brief report: chimeric pigs produced from induced pluripotent stem cells demonstrate germline transmission and no evidence of tumor formation in young pigs. *Stem Cells* *29*, 1640-1643.

Wu, Z., Chen, J., Ren, J., Bao, L., Liao, J., Cui, C., Rao, L., Li, H., Gu, Y., Dai, H., *et al.* (2009). Generation of pig induced pluripotent stem cells with a drug-inducible system. *J Mol Cell Biol* *1*, 46-54.

Yoshimatsu, S., Nakamura, M., Nakajima, M., Nemoto, A., Sato, T., Sasaki, E., Shiozawa, S., and Okano, H. (2019a). Evaluating the efficacy of small molecules for neural differentiation of common marmoset ESCs and iPSCs. *Neurosci Res*.

Yoshimatsu, S., Okahara, J., Sone, T., Takeda, Y., Nakamura, M., Sasaki, E., Kishi, N., Shiozawa, S., and Okano, H. (2019b). Robust and efficient knock-in in embryonic stem cells and early-stage embryos of the common marmoset using the CRISPR-Cas9 system. *Sci Rep* *9*, 1528.

Yoshimatsu, S., Sato, T., Yamamoto, M., Sasaki, E., Nakajima, M., Nakamura, M., Shiozawa, S., Noce, T., and Okano, H. (2020). Generation of a male common marmoset embryonic stem cell line DSY127-BV8VT1 carrying double reporters specific for the germ cell lineage using the CRISPR-Cas9 and PiggyBac transposase systems. *Stem Cell Res* *44*, 101740.

Yoshimatsu, S., Sone, T., Nakajima, M., Sato, T., Okochi, R., Ishikawa, M., Nakamura, M., Sasaki, E., Shiozawa, S., and Okano, H. (2019c). A versatile toolbox for knock-in gene targeting based on the Multisite Gateway technology. *PLoS One* *14*, e0221164.

Yu, J., Hu, K., Smuga-Otto, K., Tian, S., Stewart, R., Slukvin, II, and Thomson, J.A. (2009). Human induced pluripotent stem cells free of vector and transgene sequences. *Science* *324*, 797-801.